NOTE TO USERS

Order Reduction of IIR and FIR Filters Using Control Methods with Applications in DSL Networks

Vahid Raissi Dehkordi

A thesis

in

The Department

of

Electrical and Computer Engineering

Present in Partial Fulfillment of Requirements
For the Degree of Master of Applied Science (Electrical Engineering) at
Concordia University
Montreal, Quebec, Canada

June 2005

Your file Votre référence
ISBN: 0-494-10248-9
Our file Notre référence
ISBN: 0-494-10248-9

Abstract

Order Reduction of IIR and FIR Filters Using Control Methods with Applications in DSL Networks

In this thesis, the problem of modeling a Digital Subscriber Line (DSL) network is investigated. Any changes made to the DSL network such as addition or relocation of customers may affect the performance of the overall network. Therefore, it is very useful to have a laboratory model to test the effect of every change made to the network easily. The model can also be used by service providers to test the quality of service before assigning a line to a new customer, reducing the trouble-shooting cost.

The modeling consists of extracting the magnitude response of a particular DSL channel, fitting the data to a discrete-time finite dimensional LTI model and reducing its order reasonably. The resultant filter will be a suitable model for laboratory implementations. The magnitude response of the DSL network can be computed numerically using general and small-scale models available for transmission lines. The computation can be generalized to the distributed networks.

Digital filter approximation can be accomplished using the conventional methods. A gradient-based method is also proposed in order to generate a FIR filter. The model order reduction is performed using Balanced Realization technique which is applicable to all stable finite dimensional LTI models. It is also accomplished by minimizing either mean-squared error or infinity norm of error.

The performance of each method is evaluated using standard test loops. A reasonable range of model order for each test loop is also discussed based on the

configuration of each loop, which can be used as a general guide for any wired transmission network.

Acknowledgement

Thanks are due first to my supervisor, Dr. Amir G. Aghdam, for his great insights, guidance and sense of humor. Sincere gratitude goes to the faculty and staff of the Department of Electrical and Computer Engineering, Concordia University, for helping me in various ways regarding my academic work with excellent co-operation. I also thank Ms. DesLauriers for her advises and encouragements.

I also appreciate the help and support I received from my colleagues, especially Mr. Javad Lavai who helped me in various parts of my work. Lastly, I should thank many individuals and friends who have not been mentioned here personally. Maybe I could not have made it without your support.

Dedication

To my parents, for giving me life and love,

To my brother and sister, for their great support...

Contents:

Figures:

Tables:

List of Abbreviations:

ADSL	Asynchronous Digital Subscriber Line
ATM	Asynchronous Transfer Mode
AWG	American Wire Gauge
BIBO	Bounded Input Bounded Output
CO	Central Office
CODEC	Coder / Decoder
DFFT	Discrete Fast Fourier Transform
DLC	Digital Loop Carrier
DSL	Digital Subscriber Line
ECH	Echo Cancelled Hybrid
FDM	Frequency Division Multiplexing
FEXT	Far-End Crosstalk
FIR	Finite Impulse Response
FSK	Frequency Shift Keying
HDSL	High-bit-rate Digital Subscriber Line
HSV	Hankel Singular Value
IIR	Infinite Impulse Response
ISDN	Integrated Services Digital Network
LAN	Local Area Network
LTI	Linear Time Invariant
MDF	Main Distribution Frame

NEXT	Near-End Crosstalk
NID	Network Interface Device
NTE	Network Termination Equipment
PCM	Pulse Code Modulation
POTS	Plain Old Telephone System
PSD	Power Spectral Density
PSK	Phase Shift Keying
PSTN	Public Switching Telephone Network
RADSL	Rate Adaptive Digital Subscriber Line
SAI	Serving Area Interface
SDM	Space Division Multiplexing
SDSL	Synchronous Digital Transmission Line
SISO	Single-Input Single-Output
TDM	Time Division Multiplexing
VDSL	Very high-bit-rate Digital Subscriber Line
VLSI	Very Large Scale Integrated

Chapter 1

1 Introduction

1.1 DSL

Digital Subscriber Line (DSL) technology provides high bit rate transmission of digital information over telephone subscriber lines. Telephone lines can transmit data at millions of bits per second rate. This is accomplished by complex digital transmission techniques, which compensate for many transmission impairments common to telephone lines. These transmission techniques are based on some complex algorithms which have become practical by enormous processing power of digital signal processors based on VLSI circuits.

Telephone lines which were initially deployed to carry a single voice signal with a 3.4 kHz bandwidth channel, can now handle near 100 digitally compressed voice signals, or a video signal with quality similar to broadcast television. This high-speed digital transmission via telephone lines requires advanced signal processing to overcome transmission impairments due to signal attenuation, crosstalk noise from the signals present on other wires in the same cable, signal reflections, radio frequency and impulse noises.

DSL is now widely used for data transfer purposes. Different variants of it such as ADSL, SDSL, HDSL and VDSL support high data rates and are useful for different specific purposes. ADSL (Asynchronous DSL) for example, is the most widely used type of DSL communication. SDSL (Synchronous DSL), is mainly used by small businesses and VDSL (Very high bit-rate DSL) service provides both high transmission and reception speeds on short distances. This means the closer the user is to the service provider's central office, the higher its data transmission speed will be.

1.1.1 DSL History

The obsolescence of the twisted-pair telephone lines has been predicted many times. The popular belief of many telephone industry experts in the late 1980s was that most of the world's telephones would be directly connected via fiber optic lines in a few years. However, economic and logistical challenges of cable construction have delayed the arrival of the predicted photonic world. That is the reason why new wired communication services such as DSL still use the plain telephone lines as a part of their physical structure.

Voice-band modems were introduced in the late 1950s for the purpose of transmitting data through the Public Switched Telephone Network (PSTN). The word *modem* comes from *mo*dulator-*dem*odulator. The reason behind using modems is the fact that PSTN can not handle frequencies below approximately 200Hz. Un-modulated data requires transmission of frequencies approaching zero Hz. The modem transforms the

frequency characteristics of the data to resemble the voice signals that the PSTN is designed to convey. The PSTN conveys the signals in the 200-3400Hz frequency band and thus, the modulated data appear to be a normal voice call to the PSTN. A common example of this method is facsimile (or simply fax) machines which contain a voice-band modem to transmit the digital representation of a page.

One of the first modems of AT&T, Bell 103, was used for full-duplex, asynchronous teletype transmission at 300 b/s using FSK (Frequency Shift Keying). A few years later, the Bell 202 modem increased the bit-rate to 1200 b/s using half-duplex FSK transmission. In late 1973, the first true full-duplex 1200 b/s modem using PSK (Phase Shift Keying) was introduced with the name VA3400. In 1981 V.22bis yielded 2400 b/s full-duplex. V.32 introduced trellis coding and the big step of echo-cancelled transmission of information in both directions using the same frequency band, 9600 b/s full-duplex transmission. This progress was notable since modems preceding V.32 placed upstream transmission in a frequency band different from the downstream transmission (Frequency Division Multiplexing or FDM). After that, other standards like V.34 achieved bit rates as high as 33.6 kb/s by the year 1995 by using bandwidth optimization, constellation shaping and channel-dependent pre-coding.

The big step was taken in late 1996 when 56 kb/s PCM modems appeared and later became standardized by the V.90 ITU Recommendation in 1998. The PCM (Pulse Code Modulation) modems are asymmetric since they support up to 56 kb/s downstream and at most 33.6 kb/s in the upstream direction. In practice, PCM modems rarely achieve transmission rates above 50 kb/s because of limitations on transmitted power, tandem conversions and line impairments such as load coils. The PCM modem transmission rate

can exceed 33.6 kb/s by directly mapping the digital signal to the transmitted symbol without the impairment of quantizing noise, provided that there is a direct digital path without any analog conversion from the digital source to the PCM modem connected to the network end of the subscriber's line.

The PCM modem network architecture departs from the universal PSTN capability of the prior generations of voice-band modems. The PCM modem at the network end must have a direct digital connection to the analog-to-digital converter connected to the PCM modem user's telephone line. The PCM modem traverses the PSTN as a normal dial-up phone call. The PCM modem is like a DSL in that a direct digital connection from the network to the subscriber line interface is required, but differs from the DSL modem since the PCM modem call is carried as a PSTN POTS (Plain Old Telephone Service) call. Architecturally, PCM modems reside in a middle ground between DSL and traditional voice-band modems. PCM modems can utilize up to 4 kHz of bandwidth.

The fundamental limit of voice-band modems is the voice *co*der/*dec*oder (CODEC) that is located at the local telephone switch or digital loop carrier (DLC) terminal. The CODEC converts the analog signals on the phone line to a 64 kb/s digital representation using pulse code modulation. A voice-band modem whose signal is carried in a PSTN voice call cannot exceed the 64 kb/s bit rate.

With ITU Recommendations V.70 and V.61, voice-band modems can support simultaneous data and digitized voice via a PSTN call. V.70, using V.34 modulation and G.729 Annex A voice coding, can simultaneously convey 8 kb/s coded voice and

approximately 20 kb/s data using a single PSTN call. Because G.729 Annex A provides for silence detection, a higher data rate can be achieved during periods of silence.

Data compression techniques such as the one specified in ITU Recommendation V.42, can achieve a data rate higher than twice as much as the modem rates discussed above. However, highly random data (such as some binary files and digitized video) curtail the benefit of data compression. Data compression can also be applied to DSL, for example in ISDN with two B channels where the data throughput increases from 128 kb/s to 300 kb/s by using data compression. When data compression is used, it is usually performed on the digital information prior to the DSL transceiver. The impact of transmission bit error may be magnified by data compression.

The fundamental difference between voice-band modems and DSL systems is that voice-band modems operate over an end-to-end PSTN connection, but the DSL operates over a local loop. The voice-band modem transmission path consists of the local loop for a user, a local central office, trunk facilities which in some cases may reach thousands of miles, another central office which serves another customer and at the end a local loop serving another user. In contrast, the DSL transmission path consists of only one local loop from the user site to the nearby central office.

1.1.2 Telephone Network

The twisted-pair infrastructure or loop plant connects customers to the telephone company. It was designed to provide economical and reliable POTS. A loop plant

intended for operation of DSLs and POTS would have been designed quite differently. Local loop design practices have changed relatively little over the past 20 years. The primary changes have been the use of longer-life cables and some reduction in loop lengths via the use of Digital Loop Carrier (DLC). However, DSLs must cope with the huge base of loop plant which in some cases is about 75 years old.

The term 'loop' refers to the twisted-pair telephone line from a central office to the customer. This term originates from current flow through a looped circuit from the central office on one wire and returning on another wire.

The overall telephone network distribution is shown in Figure 1-1. Large central offices may serve over 100000 telephone lines and they all terminate at the Main Distribution Frame (MDF) in the central office. Feeder plant cables lead from the central office to the Serving Area Interface (SAI) which serves 1500 to 3000 lines. The loop plant consists of twisted wire pairs that are contained within a protective cable sheath. In some places the wires are twisted in four-wire units called quads. Within the central office, cables from switching and transmission equipment lead to the MDF which is a large wire cross-connect frame, where jumper wires connect the central office equipment cables to the outside cables. The MDF allows any subscriber line to be connected to any port of any central office equipment. Cables leaving the central office are called feeder cables and contain around 10000 wire pairs. The feeder cables extend from the central office to the wiring junction and interconnection point, SAI. The SAI contains a small wire jumper panel that permits the feeder cable pairs to be connected to any of several distribution cables. The SAI is at most 3000 feet from the customer premises and typically serves 1500-3000 units. The SAI contains only a wiring cross-connect field and

no active electronics. The loops emanating from the SAI to the customer are sometimes called the distribution plant [38].

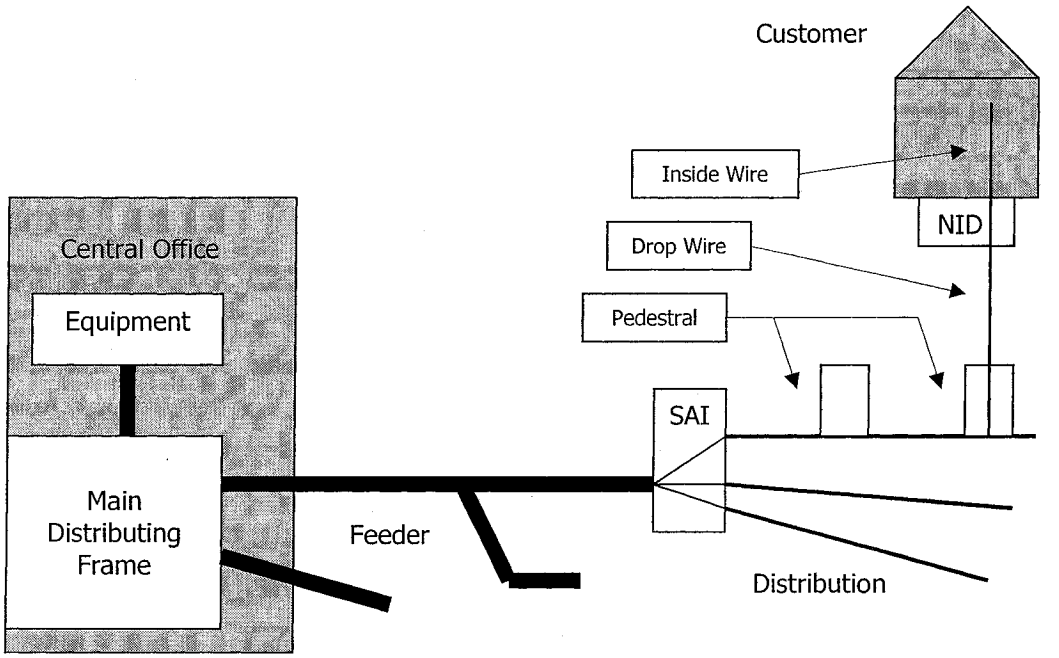

Number of loops	20000 to 160000	Around 10000	1500 to 3000	25 to 1000

Figure 1-1: Overall telephone network distribution

Distribution cables contain 25 to 1000 pairs. For small residential areas, the distribution cables lead to the drop wire that serves each customer. The distribution cable connects to the drop wires via a distribution terminal which typically serves four to six units. The drop wire connects to the inside wire via the Network Interface Device (NID) or Network Termination Equipment (NTE). Inside wire is often two twisted pairs of 24

American Wire Gauge (AWG) although wide range of wiring practices may be found inside the customer premises.

1.2 Performance of Service

The distribution of DSL service is more complicated than what described above. The DSL network should be distributed in such a way that it can support all potential users. This goal is achieved by using bridge taps. A bridge tap is a technique used in telephone installation that taps the user into a line that runs past user's premises rather than terminating there. The line does not go to anyone else's premises and it just ends somewhere up the road. This technique makes it very easy to provide service because when a user's location changes (moving, demolishing, etc.), the phone company can move the tap up or down the line in order to support more users or just manipulate existing users. It is important to remember that the end of the line is not terminated at any user's premises. Therefore, it can act like a huge antenna ready to pick up interference. The most important effect of this non-terminated line segment is that it can disturb the originally transmitted signal by reflecting the received signal, which causes the original signal to receive out-of-phase echoes.

With the different configurations mentioned above and the problems brought mainly because of bridge taps, it is of interest to have an estimation of the frequency behavior of the distribution network. To be more precise, it is important to know how the changes made in tap configuration (number of taps, their location and length) affect the

performance of DSL system since DSL technology uses variable bit rate signal processing technique. In other words, the performance of service for each end-user depends on the frequency response of the path the signal takes to reach the user.

There are some models for the frequency response of any given line configuration. If the frequency response is not satisfactory, i.e. the corresponding performance of service is poor, it may be necessary to change the line configuration which can be done in a small or a large scale. It means that the change required can be either as small as changing the location of a single tap for a single end-user or as large as changing the whole bridge tap serving the area.

Regardless of the scale of changes, it is hard to implement them in general because the communication network is an underground set-up. Therefore, it can be costly to verify and possibly change the physical configuration. The transmission line model allows the DSL network managers to have a better insight about the performance of a local network area without performing any test. Transmission lines can be modeled as digital filters which are suitable for software simulations and hardware implementations. The performance of service can then be estimated through simulations by using the frequency response of the transmission lines computed for any given configuration. It allows the service providers to verify whether the existing configuration is suitable for a DSL service.

In this thesis, the frequency characteristics of a transmission line with any configuration is obtained by using digital filters in order to simulate the frequency response of the DSL network using digital filters in a lab environment. Digital filters are classified as being either Infinite Impulse Response (IIR) or Finite Impulse Response

(FIR). FIR filters have a simple structure, but may require high orders to meet any given specifications. Several procedures for obtaining FIR approximation for IIR filters exist in the literature, such as the Fourier series method with windows, the Discrete Fast Fourier Transform (DFFT) method with windows, optimization methods, etc.

1.2.1 Windowing Technique

Several windowing techniques have been developed in the past few decades for obtaining FIR models for digital filters. Some of the most popular windows used in digital signal processing are rectangular, triangular, Hanning, Hamming, Blackman and Kaiser. Rectangular and triangular windows have simple structures but lack accuracy in terms of model error. Blackman and Kaiser windows, on the other hand, are commonly used in practice when a FIR model with a sufficiently small approximation error is required [18].

Because of the periodicity of the frequency response of a digital system, its transfer function can be determined using the Fourier series method. The coefficients of this Fourier series are coefficients of the impulse response of the filter. If the number of nonzero terms in the series expansion is finite, the filter is FIR and if it is infinite, the filter is IIR. In order to obtain a physically realizable FIR model from an IIR filter, the resulting Fourier series must be truncated by terminating the expansion with a finite number of terms. One way of limiting the number of terms in the series expansion is to terminate the series at a given point. However, this technique may result in poor

approximation if the number of terms is not sufficiently large, particularly in the vicinity of sharp transitions in frequency domain, making the method unsatisfactory for many standard types of filters. This effect due to direct truncation of discontinuous filters is known as the Gibb's phenomenon, which is simply described as the existence of some percentage of overshoot, undershoot and ripple before and after an approximated discontinuity. The process of terminating the series after a finite number of terms can be considered as multiplying the infinite length impulse response by a finite width window function. In other words the window function determines the duration of the original impulse response that one could see, and that is why it is called a "window".

The history of windowing functions goes back to 50's and 60's, when the first windowing functions were tested, using early generation of computers. However, the windowing functions were mainly developed and implemented in 60's and 70's, notably by Kaiser in 1963 and by Hamming in 1977. There are complete reviews about windowing function mostly published in 70's and 80's, notably by Fredric J. Harris and later by A. Nuttall. Since then, several variants of windowing functions are proposed which have better performance compared to the original windowing functions and are useful for different applications [17].

1.2.2 Control-based Model-Order Reduction

From the control point of view, the model-order reduction consists of reducing the order of a system without exactly dealing with its impulse response, meaning that the

model is treated as a system rather than a digital filter. In other words, model-order reduction can be applied to any control system regardless of it representing a digital filter or a control system. Several methods are proposed for this purpose, which essentially reduce the order of system by eliminating some of the states of the system which have smaller effect in the overall behavior of the system [16].

The main question is how to find the best approximate model for a system. To answer this question, the closeness of the reduced-order model to the original one should be measured using a performance index or cost function. The performance index can be defined based on either the time response or the frequency response of the system, with possible weighting functions. Singular perturbation and dominant modes approaches are presented by Davison [8] which deal with removing the states which have less effect among all the states, or directly removing the poles of the system which are far from the origin in the left half s-plane and hence have less effect on the response of the system compared to the other poles.

The balanced realization method proposed by Moore [26] provides an attractive framework for reducing the order of a LTI system. Balanced realization theory states that for a stable, LTI dynamic system, a coordinate transformation exists such that the controllability and observability gramians of the transformed system are equal and diagonal. Such systems are called balanced and are characterized by having states that are equally controllable and observable. The relative degree of controllability/observability among the states is given by the Hankel Singular Values (HSV). Thus, states corresponding to large HSVs are highly controllable/observable and contribute significantly to the input/output behavior of the system. In contrast, states associated with

small HSVs are weakly controllable/observable and contribute little to the input/output behavior of the system. Therefore, a model order reduction is accomplished by retaining only those states with large HSVs and truncating states associated with small HSVs. Other attractive features of the theory are the easily obtainable error bound [10], [15] and guaranteed stability for the reduced-order system [26], [33].

The thesis is organized as follows. Chapter 2 discusses different DSL transmission modes and their purpose. The generic twisted pair transmission model is then introduced which is followed by the modeling of the transmission line by introducing its simplified circuit model. Finally, a numerical method for computing of the frequency response of the transmission line is given.

Chapter 3 provides a brief review on FIR filters. The concepts of infinity-norm and mean-squared error are discussed and an algorithm is proposed in order to find a FIR filter which approximates a given magnitude response in mean-squared sense.

Chapter 4 discusses different techniques for reducing the order of digital filters. It introduces methods in control theory which were initially proposed for reducing the order of control systems. Preserving the stability of the system and also giving a measure of closeness between original and reduced-order systems. In order to achieve this goal, balanced realization technique is used as an efficient method for model order reduction. Also a computationally efficient method is proposed in order to reduce the order of an IIR filter using long division followed by the balanced realization technique. Finally, a general survey is made on some standard DSL test loops and the results are discussed thoroughly.

Chapter 2

2 DSL Architecture

In this chapter different DSL transmission modes are discussed. The generic twisted pair transmission model is then introduced and the standard terms such as American Wire Gauge (AWG) are defined. Bridge taps are introduced and their effects on the behavior of a DSL loop are discussed in detail. Modeling of the transmission line is accomplished by finding the simplified circuit model of the overall transmission line between transmission and reception points, and using then the small-piece model of the line. The model parameters are then provided which lead to a numerical method for computing the frequency response of the transmission line. Finally, the Power Spectral Density (PSD) of ADSL is provided which will be used later as a weighting function.

2.1 Transmission Modes

There are several transmission modes used in different types of DSL, depending on application requirements and channel characteristics [38]:

- By direction:
  - Simplex: This kind of transmission is permanently one way from a source to a destination. Examples of simplex transmission include radio broadcast and security alarm circuits. Virtually all DSL applications require two-way transmission. Therefore, Simplex transmission is usually not used for DSLs. T1 lines are comprised of two simplex lines sending in opposite directions.
  - Half-Duplex: Periodically transmits from station A to station B and at other times in the opposite direction, meaning that at any point in time information is sent in one direction.
  - Full-Duplex: Sends information continuously in both directions on the same wire pair. Examples include traditional voice telephones, voice-band modems and HDSL. An Echo-Cancelled Hybrid (ECH) method is often used to allow both directions to use the same frequency band.

- By timing:
  - Synchronous: Sends bits at a continuous rate. DSL receivers usually derive their timing from the periodicity of the received bit transitions. Synchronous and asynchronous transmission may apply for simplex, half-duplex and full-duplex transmission. In general, DSLs use synchronous, not asynchronous transmission.
  - Asynchronous: Sends units (characters or blocks) with a unique flag to mark the start of each unit. Asynchronous Transfer Mode (ATM) works in

synchronous mode at bit level, but the start point of each cell may be at any idle bit. Thus, ATM is asynchronous at the cell level.

- By channel division:
  - Time Division Multiplexing (TDM): This is the most commonly used method to convey multiple channels of information. Information is divided into fixed-length frames with a fixed number of bits.
  - Frequency Division Multiplexing (FDM): Different frequency bands are allocated for each channel, i.e. all informations are sent at the same time, but in different frequency bands. One application of this method is the use of one frequency band for upstream data and another frequency band for downstream information in ADSL systems.
  - Space Division Multiplexing (SDM): This method simply puts each channel on a separate set of wires. This transmission mode is suitable for data transmission over distances measured in centimeters, but the cost rises rapidly because of the number of wires and additional transceivers. As an example, HDSL systems use two or three lines to achieve longer line distances.

- By topology:
  - Point-to-point: DSL is a point-to-point transmission system. One transceiver to each of the two ends of a pair of wires. One end can be, for

example, located at a telephone company site and the other end can be placed in customer's premises.

- Point-to-multipoint: This consists of a central station transceiver, which communicates with multiple directly connected terminals. Note that terminals do not directly communicate with each other. Local Area Network (LAN) is an example of this topology.

Table 2-1 shows different types of DSL services and their characteristics:

Table 2-1: Different types of DSL and their usage

Type	*Transfer Rate*	*Mode*	*Note*
ISDN	160kbps	Full Duplex	The very first implementation of voice/data transmission
HDSL	1.544-2.048Mbps	Full Duplex/Dual Simplex/Dual Duplex	Bit error rate around 10-7
ADSL1	Downstream 1.5Mbps Upstream 16kbps	Asymmetric Full Duplex with FDM or ECH	One MPEG-1 channel
ADSL2	Downstream 3Mbps Upstream 16kbps		Two MPEG-1 channels
ADSL3	Downstream 6Mbps Upstream 64kbps		One MPEG-2 channel
RADSL	Downstream 7-10Mbps Upstream 512-900kbps		
VDSL	Downstream up to 52Mbps	Asymmetric Full Duplex	Short loops for optical fibers

2.2 Generic Twisted Pair Transmission Model

Figure 2-1 shows a simple model of the line configuration used in a generic DSL data transmission system:

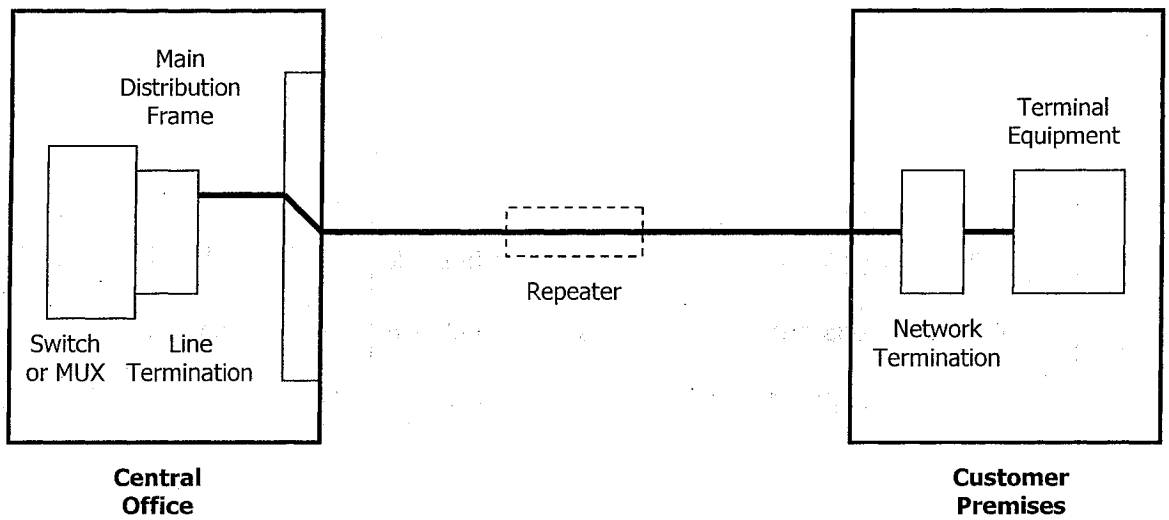

Figure 2-1: Twisted pair transmission model

Line Termination represents the DSL modem at the network end of the loop and Main Distribution Frame represents a wire cross-connection field used to connect any loop to any Central Office (CO) equipment.

The local loop transfers voice/data between CO and Customer Premises (i.e. ordinary internet users). In some long loops, Repeaters are used in the middle of local

loop in order to make transmission on long loops possible. It should be mentioned that Repeaters are not needed in majority of lines.

In Customer Premises, Network Termination represents the DSL modem at the customer end of the local loop and Terminal Equipment can be any end-user equipment such as personal computer or a telephone.

2.3 Frequency Response Derivation

DSL transmission network from service provider's office to end-user's place has a frequency response which depends on network architecture. It depends on the line length, the number, the place and length of bridge taps – branches which connect other users to the main line – also different types of line used (AWG 22, AWG 24 or AWG 26, etc.) and some other parameters.

2.3.1 Wire Gauge

AWG or American Wire Gauge is a measure of wire diameter. Most of the loop plants in the United States follow the 1300 ohm resistance design, which implies that the first 10000 feet of cable from the CO is 26 AWG. After this point, successively heavier

wire is used to avoid excessive loop resistance. Very long loops may use 22 or 19 AWG wires.

Wire is commonly spliced in 500 feet segments. As a result, signal reflection can result from the impedance change due to splicing one wire gauge to a different wire gauge. Longer loops may have several changes in wire gauge. The degree of transmission impairment caused by a gauge change is debated. Most experts believe that DSLs with echo cancellers tolerate gauge changes and the effects of a gauge change are small enough to be ignored. The following table shows the resistance per mile of a loop at a temperature of 70°F as the loop resistance varies with temperature. The loop resistance is the total of the round-trip circuit for one conductor out and one conductor back [36-37].

Table 2-2: Measurement specifications of AWG lines

AWG	Metric Size (mm)	Loop Resistance (Ω/mile)
28	0.32	685
26	0.4	441
24	0.5	277
22	0.63	174

2.3.2 Bridge Tap

In some countries, there is a common practice of splicing a branching connection called a bridge tap onto a cable. A bridge tap is a length of wire pair that is connected to a loop at one end and is unterminated at the other end. Sometimes several bridge taps exist

on a loop. Bridge taps may be located near either end or at an intermediate point. One reason for using a bridge tap is that it allows all the pairs in a cable to be used or reused to serve any customer along the cable route. The reflection of signals from the unterminated bridge taps results in signal loss and distortion. The adaptive equalizer and echo canceller which exist in many DSL lines, partly reduce the transmission impairment caused by bridge taps. The worst-case bridge tap is a heavy-gauge tap of length that is equal to one quarter of the wavelength of any used transmission frequencies which causes an additional loss of 3-6 dB. The reflections from a quarter-wavelength tap are 180 degrees out of phase from the primary signal frequency and thus partly cancel the signal. DSLs can tolerate multiple bridge taps provided that the combined signal loss due to loop length and bridge taps is within the system's loss budget. The effect of bridge taps can actually be evident at several frequencies.

Figure 2-2 shows what happens in presence of a bridge tap. When the transmitted pulse reaches the bridge tap, it divides its energy between the two paths. The forward pulse continues to go while the other pulse goes through the bridge tap and reflects from the unterminated tap end. Again at the intersection, the reflected pulse divides its energy between two forward and backward paths, causing multiple echoes.

Depending on the shape of transfer function curve, different bit rates are assigned for each frequency band, meaning that more bits are transmitted in frequency bands which have higher amplitude and the number of assigned bits gradually decreases as frequency response gets weaker in higher frequencies. This method of assignment provides an optimum capacity for data transmission on normal telephone lines. In normal voice conversations, only a bandwidth of 4 KHz is used, but with the method mentioned

above, a wide bandwidth of about 1 MHz is used which provides high bit rates as well as maintaining regular voice conversations. Therefore, it is very important to estimate the frequency response of a transmission line configuration in order to have the maximum efficiency.

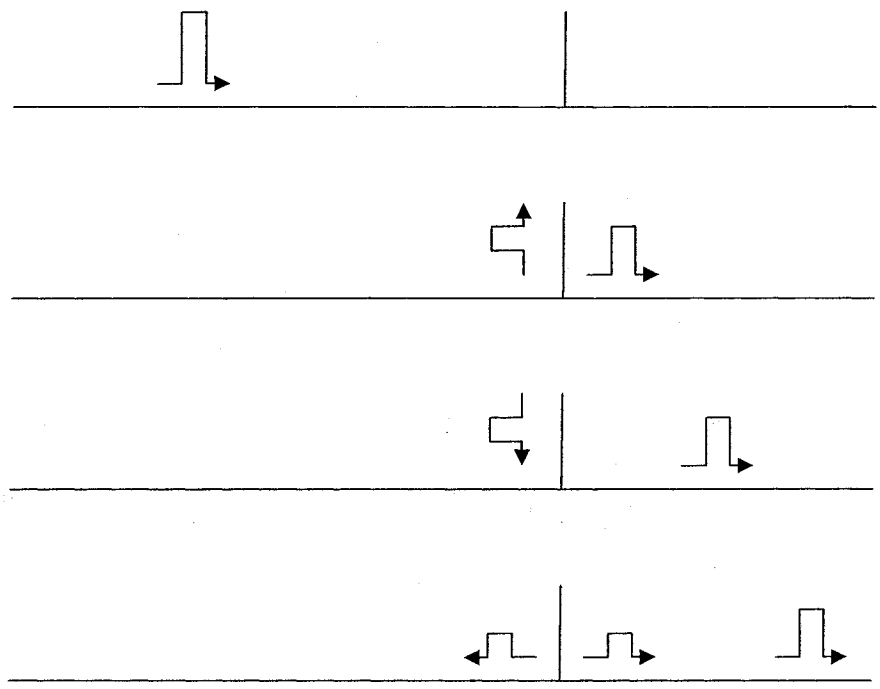

Figure 2-2: The effect of bridge tap on transmitted signal, (a) transmitted signal passes through the line, (b) it is divided into two parts with divided energy; (c) the part of signal in bridge tap is reflected; (d) the reflected signal is divided again into two parts.

2.3.3 Circuit Modeling

The overall line is modeled as shown in Figure 2-3:

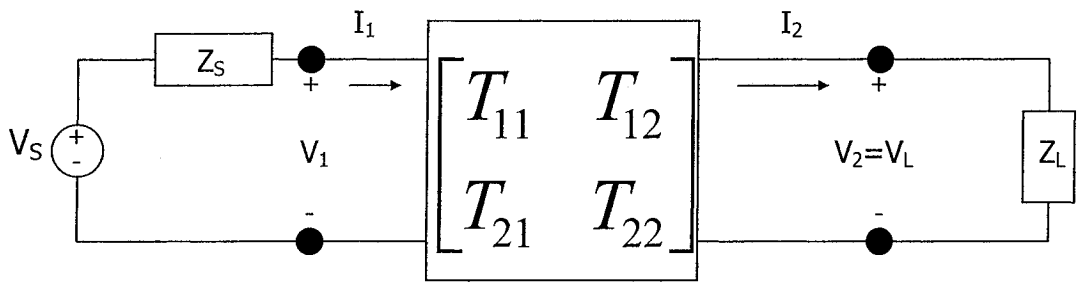

Figure 2-3: The simplified circuit model of the overall transmission line between transmission and reception points.

The T-matrix shown above satisfies the following equation between voltages V_1 and V_2 and currents I_1 and I_2, with respect to their polarities and directions [38]:

$$\begin{bmatrix} V_1 \\ I_1 \end{bmatrix} = \begin{bmatrix} T_{11} & T_{12} \\ T_{21} & T_{22} \end{bmatrix} \begin{bmatrix} V_2 \\ I_2 \end{bmatrix} = \Phi \cdot \begin{bmatrix} V_2 \\ I_2 \end{bmatrix} \tag{2.1}$$

where:

$$\Phi = \begin{bmatrix} T_{11} & T_{12} \\ T_{21} & T_{22} \end{bmatrix}$$

The parameters T_{11}, T_{12}, T_{21} and T_{22} can be obtained from the following equations:

$$\begin{aligned} T_{11} &= \left.\frac{V_1}{V_2}\right|_{I_2=0} \\ T_{12} &= \left.\frac{V_1}{I_2}\right|_{V_2=0} \\ T_{21} &= \left.\frac{I_1}{V_2}\right|_{I_2=0} \\ T_{22} &= \left.\frac{I_1}{I_2}\right|_{V_2=0} \end{aligned} \tag{2.2}$$

Parameters T_{11}, T_{12}, T_{21} and T_{22} are, in fact, frequency dependent. If all different segments of a transmission line are described by the matrix representation of (2.1), then the overall matrix representation for the above model can be obtained as follows:

$$\begin{bmatrix} V_1 \\ I_1 \end{bmatrix} = \Phi \cdot \begin{bmatrix} V_N \\ I_N \end{bmatrix}, \quad \Phi = \prod_{i=1}^{N-1} \Phi_i \tag{2.3}$$

So the overall Φ-matrix is calculated by multiplying the Φ-matrices for all segments. The transfer function from V_S to V_L can now be computed using the parameters T_{11}, T_{12}, T_{21}, T_{22} and also Z_S and Z_L [40].

For calculating the transfer function, each small piece of the transmission line with length *dx* is modeled as shown below:

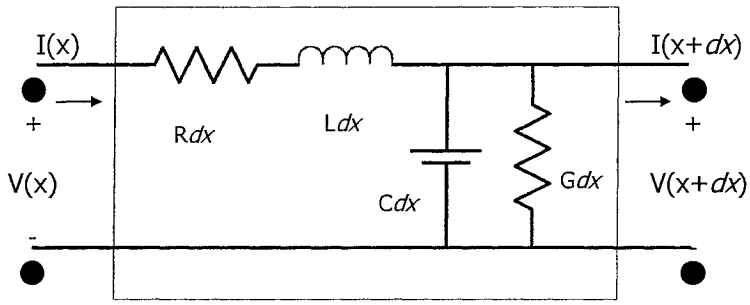

Figure 2-4: Model of a small segment of transmission line

where R, L, C and G represent resistance, inductance, capacitance and conductance per mile, respectively. These parameters are functions of frequency and line type. It is to be noted that in high frequencies, the overall network no longer behaves as a lumped circuit and therefore cannot be modeled by a fixed set of elements [7]. The equations for RLCG parameters are as follows [39]:

$$
\begin{aligned}
R(f) &= \frac{1}{\frac{1}{\sqrt[4]{r_{0c}^4 + a_c \cdot f^2}} + \frac{1}{\sqrt[4]{r_{0c}^4 + a_s \cdot f^2}}} \\
L(f) &= \frac{l_0 + l_\infty \left(f / f_m \right)^b}{1 + \left(f / f_m \right)^b} \\
C(f) &= c_\infty + c_0 \cdot f^{-c_e} \\
G(f) &= g_0 \cdot f^{g_e}
\end{aligned}
\tag{2.4}
$$

in which the parameters r_{0c}, a_c, r_{0s}, a_s, l_0, l_∞, b, f_m, c_∞, c_0, c_e, g_0 and g_e are obtained experimentally through measurement tests. These parameters vary for

different line gauges. The nominal values for 26 and 24-Gauge twisted pairs are given in the following table [39]:

Table 2-3: The nominal values for parameters used in calculation of resistance, inductance, capacitance and conductance of (a) AWG 26; and (b) AWG 24 transmission lines.

Resistance	r_{0c} 286.17578 Ω/km	r_{0s} ∞ Ω/km	a_c 0.1476962	a_s 0.0
Inductance	L_0 675.36888 μH/km	l_∞ 488.95186 μH/km	b 0.92930728	f_m 806.33863 kHz
Capacitance	c_∞ 49 nF/km	c_0 0.0 nF/km	c_e 0.0	
Conductance	G_0 43 nS/km	g_e 0.70		

(a)

Resistance	r_{0c} 174.55888 Ω/km	r_{0s} ∞ Ω/km	a_c 0.053073481	a_s 0.0
Inductance	L_0 617.29539 μH/km	l_∞ 478.97099 μH/km	b 1.1529766	f_m 553.760 kHz
Capacitance	c_∞ 50 nF/km	c_0 0.0 nF/km	c_e 0.0	
Conductance	G_0 234.87476 fS/km	g_e 1.38		

(b)

The following two joint differential equations describe the relation between the voltages and currents of the two-port network at any point x:

$$\begin{aligned} -\frac{dV}{dx} &= (R + j\omega L)\cdot I \\ -\frac{dI}{dx} &= (G + j\omega C)\cdot V \end{aligned} \tag{2.5}$$

V and I are phasor quantities at any given frequency $\omega = 2\pi f$. Taking derivative of (2.5) and substituting from (2.5), one can obtain:

$$\frac{d^2V}{dx^2} = \gamma^2 \cdot V$$
$$\frac{d^2I}{dx^2} = \gamma^2 \cdot I \tag{2.6}$$

where

$$\gamma = \alpha + j\beta = \sqrt{(R + j\omega L)(G + j\omega C)} \tag{2.7}$$

is called the propagation constant of the line. The solution to this differential equation is modeled as the sum of two opposite direction voltage/current waves:

$$V(x) = V_0^+ \cdot e^{-\gamma x} + V_0^- \cdot e^{\gamma x}$$
$$I(x) = I_0^+ \cdot e^{-\gamma x} + I_0^- \cdot e^{\gamma x} \tag{2.8}$$

Another transmission line parameter called characteristic impedance is defined as the ratio between forward (or backward) voltages and currents, i.e.:

$$Z_0 = \frac{V_0^+}{I_0^+} = -\frac{V_0^-}{I_0^-} = \sqrt{\frac{R + j\omega L}{G + j\omega C}} \tag{2.9}$$

Thus, for a segment of line with length d, the following T matrix describes the relation between the voltage/current pairs at both ends of the segment:

$$\begin{bmatrix} \cosh(\gamma d) & Z_0 \sinh(\gamma d) \\ 1/Z_0 \sinh(\gamma d) & \cosh(\gamma d) \end{bmatrix} \tag{2.10}$$

In the case of a segment with open ends at one side (a bridge tap), the matrix will differ from the general form shown above since backward direction voltages and currents do not exist anymore:

$$\begin{bmatrix} 1 & 0 \\ 1/Z_0 \tanh(\gamma d) & 1 \end{bmatrix} \tag{2.11}$$

In order to obtain the overall matrix representation of the transmission line, one should calculate individual T-matrices for each segment of the line, when each has its own characteristic model. For example, when the type of the wire used for a segment changes, a new T-matrix should be composed for that segment with a different wire type. Since each line segment has its own characteristic impedance and propagation constant and they are functions of frequency, the overall T-matrix will have a complex set of functions of frequency. Therefore, the parameters of the transfer function from the source to the load will also be frequency-dependent.

The overall transfer function will be calculated using the following equation:

$$\frac{V_L(f)}{V_S(f)} = \frac{Z_1}{Z_1 + Z_S} \cdot \frac{Z_L}{T_{11}Z_L + T_{12}} \qquad Z_1 = \frac{T_{11}Z_L + T_{12}}{T_{21}Z_L + T_{22}} \tag{2.12}$$

where Z_1 represents the input impedance of T-matrix.

Example 2.1: Consider two transmission lines, one with bridge tap and the other one without bridge tap. Both lines are of type AWG 26 and the second line has a bridge tap right in the middle:

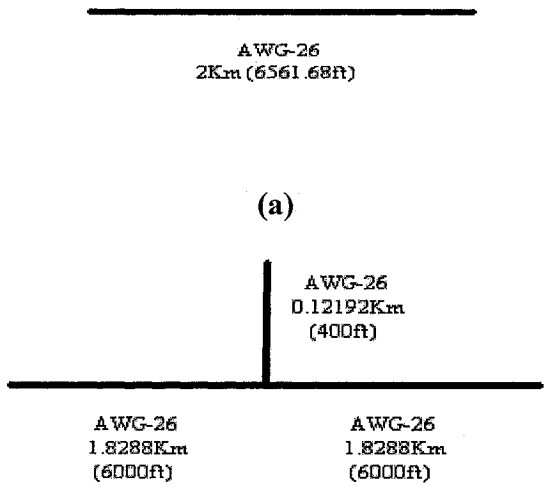

Figure 2-5: Two line configurations used in Example 2.1, (a) without a bridge tap; (b) with a bridge tap

The magnitude response of the line configurations of Figure 2-5(a) and (b) are given in Figures 2-6 and 2-7, respectively.

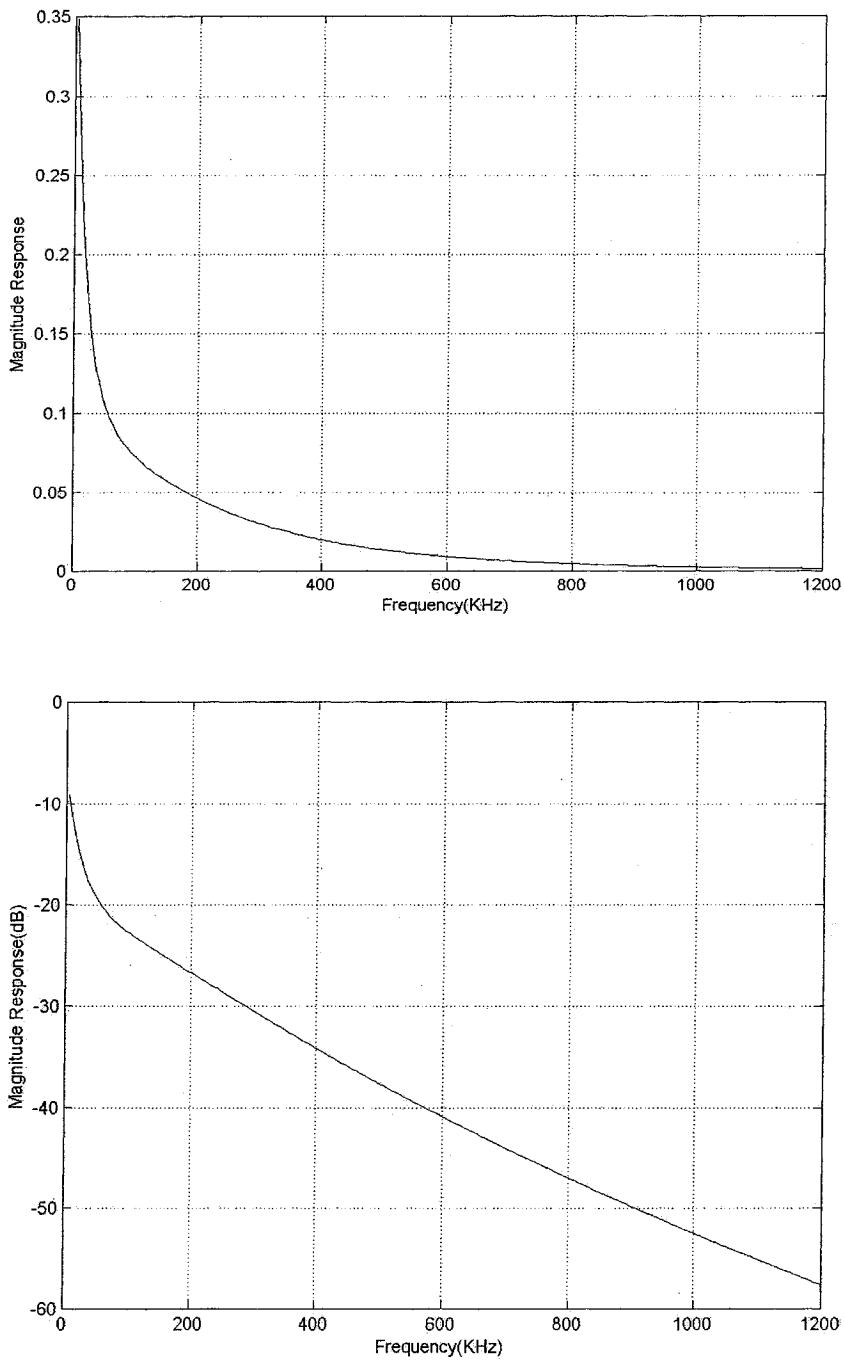

Figure 2-6: The magnitude response of the DSL line configuration given in Figure 2-5(a)

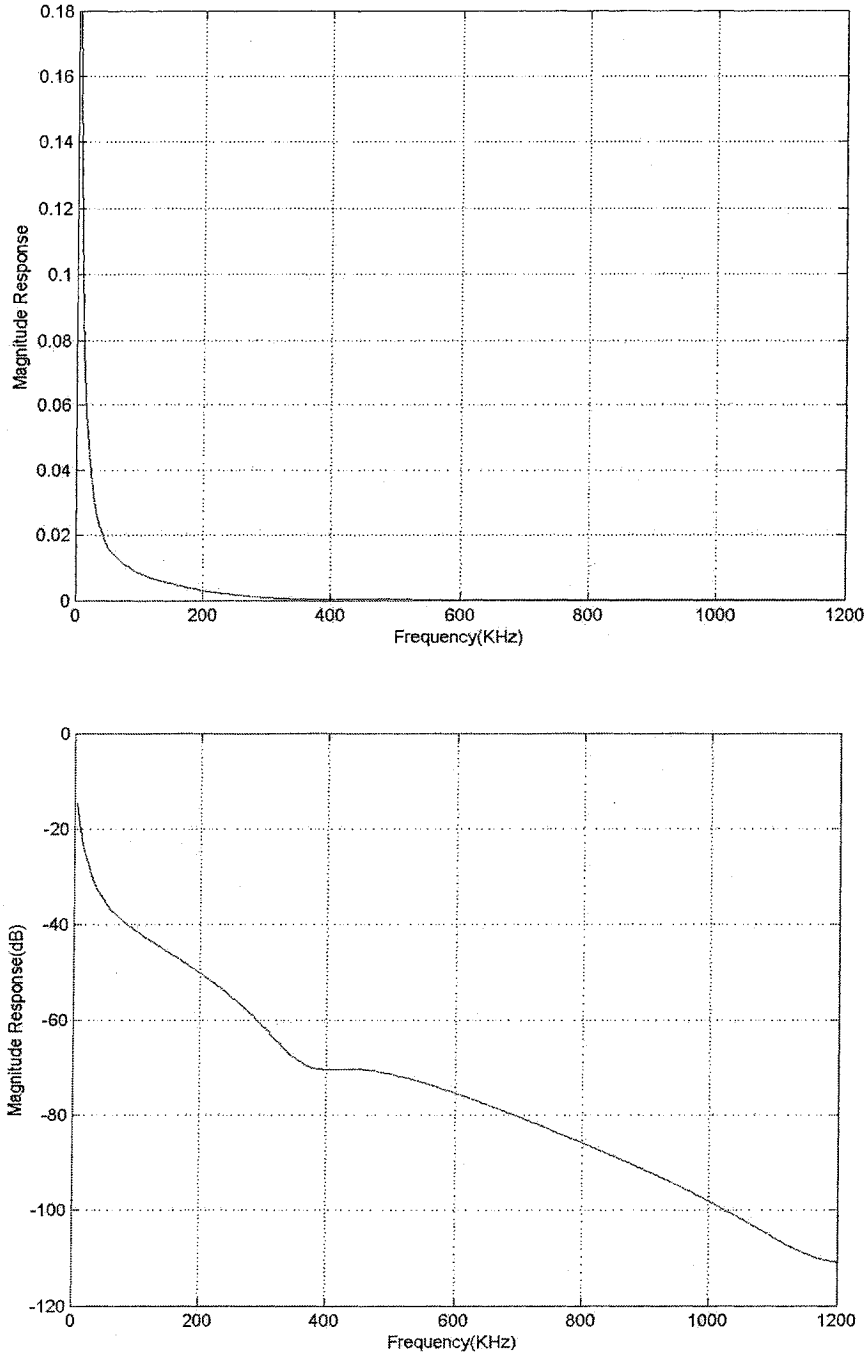

Figure 2-7: The magnitude response of the DSL line configuration given in Figure 2-5(b)

It can be seen from the above figures that the bridge tap generates periodic notches in the magnitude response of the line, which is caused by the signal returned

from the unterminated end. The location of notches in the magnitude response depend on the length of bridge tap (and the corresponding gauge) and for this example, they are at 400kHz, 1.2MHz, etc. This rough behavior caused by bridge taps can result in signal loss, which can in turn cause insufficient data transfer capacity. Therefore transmission line's frequency behavior estimation is important and can improve the performance of the overall network.

2.3.4 Non-uniform Frequency Distribution

To find a model for the transmission line in the frequency domain, the frequency response should be known at a set of points in the frequency axis. In other words, the frequency response is to be determined at certain number of frequency points. The frequency points can be chosen in either a uniform or a non-uniform fashion. This is important since for some algorithms which will be discussed later, some frequency ranges are of more interest and therefore more points need to be assigned in those frequency ranges, which result in a non-uniform frequency grid.

This non-uniform assignment is based on the frequency properties of different types of DSL. For example, most ADSL systems use FDM transmission technique, which places upstream transmission in a distinct frequency band from the downstream transmission, to prevent self-crosstalk as shown in Figure 2-8(a). The guard band is necessary to facilitate filters that prevent POTS noise from interfering with the digital transmission. On the other hand, some ADSL systems use an ECH transmission

technique, where the upstream frequency band resides within the downstream band. By overlapping the bands, as shown in Figure 2-8(b), the total transmitted bandwidth may be reduced. However, the ECH is subject to self-crosstalk, and its implementation involves more complex digital signal processing. There is some debate as to whether the digital complexity is offset by simplification of the analog front-end.

The upstream performance of FDM ADSL is much better than that of ECH ADSL since there is no cross-talk at the CO end. However, the wider downstream bandwidth of ECH ADSL permits better downstream performance, specially in shorter loops.

The performance of symmetric DSL is primarily limited by self Near-End Crosstalk (NEXT). Compared to the symmetric DSL, ADSL overcomes self NEXT at the costumer end simply by reducing the source of the self NEXT. By reducing the upstream bit rate, the upstream channel may be positioned to minimize crosstalk into the downstream transmission. For ADSL, reception of the upstream channel is made easier by placing it at lower frequencies where the loop loss and crosstalk effect are smaller.

Based on the examples given on the frequency distribution of DSL services, it is obvious that some frequency bands have less effect in DSL data transmission and can be ignored in modeling process. Thus for modeling purpose, one can use a simple weighting function based on the shape of PSD, e.g. the ones shown in Figure 2-8, in which more emphasis is put on active frequency bands.

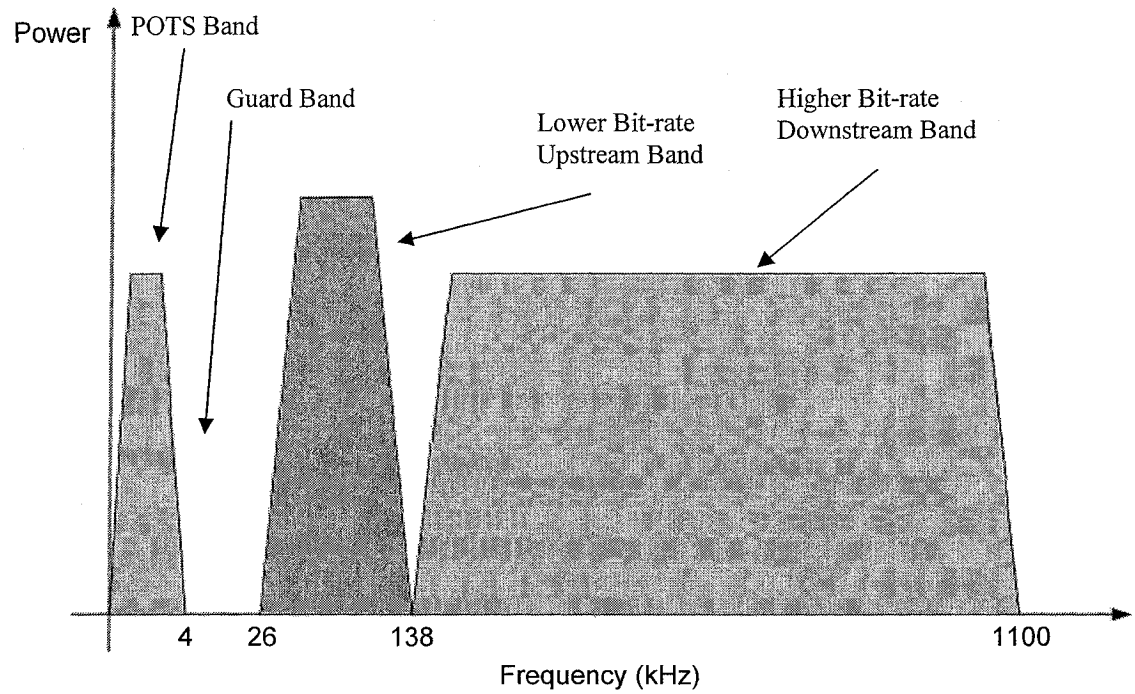

(a)

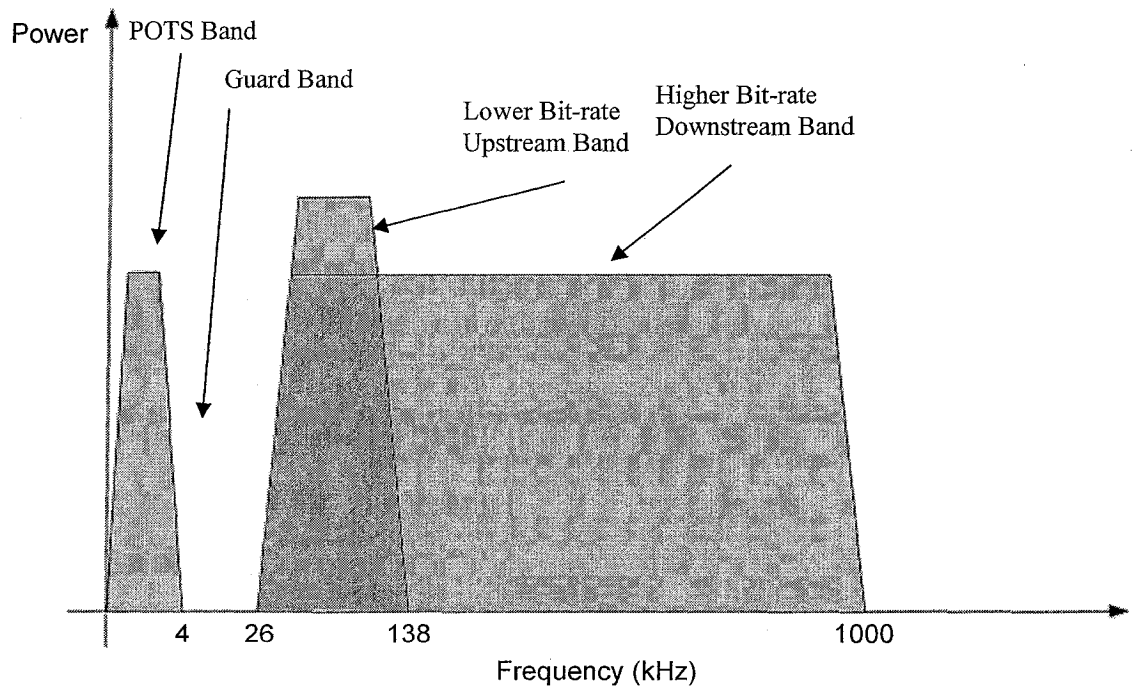

(b)

Figure 2-8: Frequency distribution or PSD of (a) FDM ADSL service, and (b) ECH ADSL service

Chapter 3

3 Digital Filter Approximation

Once the frequency response is determined at certain points on the frequency axis, it is desired to find a digital filter which approximates this discretized frequency response. The sampling frequency used for discretization of DSL systems is 4135Hz. The accuracy of this approximation is evaluated based on some optimality criteria which are usually based on the error between the original frequency response and the resultant approximate filter. The error may be defined only for the complex frequency response, or for the magnitude response only. The latter simplifies the computations significantly and also the magnitude response is usually more important in practice.

The two most popular error measurements defined for the filter design are mean-squared and ∞-norm errors [35]. Suppose that the original frequency response and the approximate one are denoted by $H(e^{j\omega})$ and $\hat{H}(e^{j\omega})$, respectively. The mean-squared error of the magnitude response is defined as:

$$\sum_{k=1}^{N}\left(\left|H(e^{j\omega_k})\right|-\left|\hat{H}(e^{j\omega_k})\right|\right)^2 \tag{3.1}$$

where ω_k, $k=1,\cdots,N$ represents the frequencies at which the magnitude response is evaluated. One can also prioritize different frequency ranges in the optimization problem

nonuniformly. As discussed earlier, the Power Spectral Density (PSD) of the DSL signal can potentially be a good weighting function in fact because it directly represents relative significance of different frequencies. Therefore, the weighted mean-squared error of the magnitude response will be defined as:

$$\sum_{k=1}^{N} W^2(k)\left(\left|H(e^{j\omega_k})\right| - \left|\hat{H}(e^{j\omega_k})\right|\right)^2 \tag{3.2}$$

The weighting function is denoted by vector W which has the same length as the number of frequency points used in the approximation. It is to be noted that the mean-squared error for the whole frequency response in general case (not just magnitude) is defined as:

$$\sum_{k=1}^{\infty} \left|H(e^{j\omega_k}) - \hat{H}(e^{j\omega_k})\right|^2 \tag{3.3}$$

The ∞-norm error for the whole frequency response is defined as follows:

$$\left|H(e^{j\omega}) - \hat{H}(e^{j\omega})\right|_{\infty} = \max\left|H(e^{j\omega}) - \hat{H}(e^{j\omega})\right| \tag{3.4}$$

3.1 Discrete-time Finite-dimensional LTI Filters

In many applications, it is desired to find the filter approximation in the discrete-time domain, using a rational transfer function:

$$H(z) = \frac{b_0 z^k + b_1 z^{k-1} + \cdots + b_{k-1} z + b_k}{a_0 z^k + a_1 z^{k-1} + \cdots + a_{k-1} z + a_k} \tag{3.5}$$

which represents a finite-dimensional Linear Time-Invariant (LTI) system. This type of discrete-time filters can be classified based on the duration of their impulse response. This will be discussed in the next two subsections.

3.1.1 IIR Filters

An Infinite Impulse Response (IIR) discrete-time filter is an LTI finite dimensional system whose impulse response has infinitely many samples. In terms of the transfer function, at least two of the coefficients a_i, $i = 0, \cdots, k$ in the denominator of the transfer function of an IIR filter are nonzero. The filter is Bounded-Input Bounded-Output (BIBO) stable if and only if all of its poles (roots of the denominator of the transfer function in (3.5)) lie within the unity circle.

3.1.2 FIR Filters

Finite Impulse Response (FIR) filters are considered as a special case of IIR filters in the sense that all of their poles are located in the origin. In other words, all coefficients in the denominator of a FIR filter are zero except a_0, i.e.:

$$H(z) = \frac{b_0 z^k + b_1 z^{k-1} + \cdots + b_{k-1} z + b_k}{a_0 z^k} \tag{3.6}$$

The coefficients b_i, $i = 0, \cdots, k$ in (3.6) are, in fact, samples of the impulse response of the system. It is to be noted that all FIR filters are BIBO stable [27].

3.2 Mean-Squared Error Approximation

Suppose that we have the magnitude response of the desired transfer function in N distinct equidistant frequency points from 0 to π rad/sec and we want to find a causal FIR filter with degree of M which means that there will be $M+1$ coefficients $b_0, \ldots, b_M$. The approximation is done with sole respect to the magnitude response. Therefore the phase response is considered totally arbitrary and no special condition, e.g. linear phase, is applied.

$$\hat{H}(e^{j\omega}) = b_0 + b_1\cos\omega + \cdots + b_M\cos M\omega - j\left(b_1\sin\omega + \cdots + b_M\sin M\omega\right) \tag{3.7}$$

$$\begin{aligned}\left|\hat{H}(e^{j\omega})\right|^2 &= \left(b_0 + b_1\cos\omega + \cdots + b_M\cos M\omega\right)^2 + \left(b_1\sin\omega + \cdots + b_M\sin M\omega\right)^2 \\ &= \sum_{j=0}^{M} b_j^2 + 2\sum_{j=1}^{M}\sum_{i=0}^{j-1} b_i b_j\cos(j-i)\omega\end{aligned} \tag{3.8}$$

Let E represent the mean-squared error of the magnitude response as defined in (3.1). Since the value of the magnitude response is known at N frequency points $\omega_k = k\frac{\pi}{N}$, $k = 0,1,\cdots,N-1$, E can be calculated as:

$$\begin{aligned}E &= \sum_{k=0}^{N-1}\left[W(k)\left(\left|\hat{H}(e^{j\omega_k})\right| - \left|H(e^{j\omega_k})\right|\right)\right]^2 \\ &= \sum_{k=0}^{N-1} W^2(k)\left|\hat{H}(e^{j\omega_k})\right|^2 + \sum_{k=0}^{N-1} W^2(k)\left|H(e^{j\omega_k})\right|^2 - 2\sum_{k=0}^{N-1} W^2(k)\left|\hat{H}(e^{j\omega_k})\right|\left|H(e^{j\omega_k})\right| \\ &= \sum_{k=0}^{N-1} W^2(k)\left|\hat{H}(e^{j\frac{\pi k}{N}})\right|^2 + \sum_{k=0}^{N-1} W^2(k)\left|H(e^{j\frac{\pi k}{N}})\right|^2 - 2\sum_{k=0}^{N-1} W^2(k)\left|\hat{H}(e^{j\frac{\pi k}{N}})\right|\left|H(e^{j\frac{\pi k}{N}})\right| \\ &= \sum_{k=0}^{N-1} W^2(k)\left(\sum_{j=0}^{M} b_j^2 + 2\sum_{j=1}^{M}\sum_{i=0}^{j-1} b_i b_j\cos\left(\frac{(j-i)\pi k}{N}\right)\right) + \sum_{k=0}^{N-1} W^2(k)\left|H(e^{j\frac{\pi k}{N}})\right|^2 \\ &\quad - 2\sum_{k=0}^{N-1} W^2(k)\left|H(e^{j\frac{\pi k}{N}})\right|\sqrt{\sum_{j=0}^{M} b_j^2 + 2\sum_{j=1}^{M}\sum_{i=0}^{j-1} b_i b_j\cos\left(\frac{(j-i)\pi k}{N}\right)}\end{aligned} \tag{3.9}$$

Let B and D represent vectors containing the filter coefficients and desired magnitude response values, i.e. $D(k) = \left|H(e^{j\omega_k})\right|$. Define the function $f(B,k)$ as:

$$f(B,k) = \sum_{j=0}^{M} b_j^2 + 2\sum_{j=1}^{M}\sum_{i=0}^{j-1} b_i b_j \cos\left(\frac{(j-i)\pi k}{N}\right) \tag{3.10}$$

Equation (3.9) can then be simplified as:

$$E_N(B,D) = \sum_{k=0}^{N-1} W^2(k) f(B,k) + \sum_{k=0}^{N-1} W^2(k) D^2(k) - 2\sum_{k=0}^{N-1} W^2(k) D(k) \sqrt{f(B,k)} \tag{3.11}$$

In other words, E is a function of the vectors B and D. Using partial derivatives:

$$\begin{aligned} \frac{\partial E_N(B,D)}{\partial b_l} &= \sum_{k=0}^{N-1} W^2(k) \frac{\partial f(B,k)}{\partial b_l} - \sum_{k=0}^{N-1} W^2(k) \frac{D(k)}{\sqrt{f(B,k)}} \cdot \frac{\partial f(B,k)}{\partial b_l} \\ &= \sum_{k=0}^{N-1} W^2(k) \left(1 - \frac{D(k)}{\sqrt{f(B,k)}}\right) \cdot \frac{\partial f(B,k)}{\partial b_l} \end{aligned} \tag{3.12}$$

On the other hand, using the definition of $f(B,k)$:

$$\frac{\partial f(B,k)}{\partial b_l} = 2\sum_{j=0}^{M} b_j \cos\frac{(j-l)\pi k}{N} \tag{3.13}$$

$$\frac{\partial f(B,k)}{\partial B} = 2B \begin{bmatrix} 1 & \cos\frac{\pi k}{N} & \cdots & \cos\frac{(M-1)\pi k}{N} & \cos\frac{M\pi k}{N} \\ \cos\frac{\pi k}{N} & 1 & \cdots & \cos\frac{(M-2)\pi k}{N} & \cos\frac{(M-1)\pi k}{N} \\ \vdots & \vdots & \ddots & \vdots & \vdots \\ \cos\frac{(M-1)\pi k}{N} & \cos\frac{(M-2)\pi k}{N} & \cdots & 1 & \cos\frac{\pi k}{N} \\ \cos\frac{M\pi k}{N} & \cos\frac{(M-1)\pi k}{N} & \cdots & \cos\frac{\pi k}{N} & 1 \end{bmatrix}_{(M+1)\times(M+1)}$$

$$= 2B\left[\cos\frac{(i-j)\pi k}{N}\right]_{(M+1)\times(M+1)} = \left[\frac{\partial f(B,k)}{\partial b_0} \quad \frac{\partial f(B,k)}{\partial b_1} \quad \cdots \quad \frac{\partial f(B,k)}{\partial b_M}\right] \tag{3.14}$$

which results in:

$$\begin{aligned}
\frac{\partial E_N(B,D)}{\partial B} &= \left[W^2(0)\left(1-\frac{D(0)}{\sqrt{f(B,0)}}\right) \quad W^2(1)\left(1-\frac{D(1)}{\sqrt{f(B,1)}}\right) \quad \cdots \quad W^2(N-1)\left(1-\frac{D(N-1)}{\sqrt{f(B,N-1)}}\right)\right]_{1\times N} \\
&\times \begin{bmatrix} \frac{\partial f(B,0)}{\partial b_0} & \frac{\partial f(B,0)}{\partial b_1} & \frac{\partial f(B,0)}{\partial b_M} \\ \frac{\partial f(B,1)}{\partial b_0} & \frac{\partial f(B,1)}{\partial b_1} & \frac{\partial f(B,1)}{\partial b_M} \\ \frac{\partial f(B,N-1)}{\partial b_0} & \frac{\partial f(B,N-1)}{\partial b_1} & \frac{\partial f(B,N-1)}{\partial b_M} \end{bmatrix}_{N\times(M+1)} \\
&= \left[1 \quad 1 \quad \cdots \quad 1\right]_{1\times N} \times diag\left(\left[W^2(0) \quad W^2(1) \quad \cdots \quad W^2(N-1)\right]\right)_{N\times N} \\
&\times \left(I - diag\left(\left[\frac{D(0)}{\sqrt{f(B,0)}} \quad \frac{D(1)}{\sqrt{f(B,1)}} \quad \cdots \quad \frac{D(N-1)}{\sqrt{f(B,N-1)}}\right]\right)\right)_{N\times N} \\
&\times \begin{bmatrix} \frac{\partial f(B,0)}{\partial b_0} & \frac{\partial f(B,0)}{\partial b_1} & \frac{\partial f(B,0)}{\partial b_M} \\ \frac{\partial f(B,1)}{\partial b_0} & \frac{\partial f(B,1)}{\partial b_1} & \frac{\partial f(B,1)}{\partial b_M} \\ \frac{\partial f(B,N-1)}{\partial b_0} & \frac{\partial f(B,N-1)}{\partial b_1} & \frac{\partial f(B,N-1)}{\partial b_M} \end{bmatrix}_{N\times(M+1)}
\end{aligned} \tag{3.15}$$

In case of uniform weighting, the equation (3.15) will be simplified as:

$$\frac{\partial E_N(B,D)}{\partial B} = \left[\left(1-\frac{D(0)}{\sqrt{f(B,0)}}\right) \quad \left(1-\frac{D(1)}{\sqrt{f(B,1)}}\right) \quad \cdots \quad \left(1-\frac{D(N-1)}{\sqrt{f(B,N-1)}}\right)\right]_{1\times N}$$

$$\times \begin{bmatrix} \frac{\partial f(B,0)}{\partial b_0} & \frac{\partial f(B,0)}{\partial b_1} & \frac{\partial f(B,0)}{\partial b_M} \\ \frac{\partial f(B,1)}{\partial b_0} & \frac{\partial f(B,1)}{\partial b_1} & \frac{\partial f(B,1)}{\partial b_M} \\ \frac{\partial f(B,N-1)}{\partial b_0} & \frac{\partial f(B,N-1)}{\partial b_1} & \frac{\partial f(B,N-1)}{\partial b_M} \end{bmatrix}_{N\times(M+1)}$$

$$= \begin{bmatrix} 1 & 1 & \cdots & 1 \end{bmatrix}_{1\times N} \times \left(I - diag\left(\begin{bmatrix} \frac{D(0)}{\sqrt{f(B,0)}} & \frac{D(1)}{\sqrt{f(B,1)}} & \cdots & \frac{D(N-1)}{\sqrt{f(B,N-1)}} \end{bmatrix} \right) \right)_{N\times N}$$

$$\times \begin{bmatrix} \frac{\partial f(B,0)}{\partial b_0} & \frac{\partial f(B,0)}{\partial b_1} & \frac{\partial f(B,0)}{\partial b_M} \\ \frac{\partial f(B,1)}{\partial b_0} & \frac{\partial f(B,1)}{\partial b_1} & \frac{\partial f(B,1)}{\partial b_M} \\ \frac{\partial f(B,N-1)}{\partial b_0} & \frac{\partial f(B,N-1)}{\partial b_1} & \frac{\partial f(B,N-1)}{\partial b_M} \end{bmatrix}_{N\times(M+1)} \tag{3.16}$$

3.3 Examples

The magnitude response used here is the same as the one in Example 2.1. Several FIR filters with different orders are generated to approximate the magnitude response. These approximations are done both with and without a weighting function and the errors of all cases are summarized in a table for comparison.

For the simple case of no weighting function, the FIR filters are generated with 30 different orders, and the relative approximation error for each case is depicted in Figure 3-1. The relative mean-squared error is calculated using the following equation:

$$\frac{\sum_{k=1}^{N} W^2(k)\left(\left|H(e^{j\omega_k})\right| - \left|\hat{H}(e^{j\omega_k})\right|\right)^2}{\sum_{k=1}^{N} W^2(k)\left|H(e^{j\omega_k})\right|^2} \tag{3.17}$$

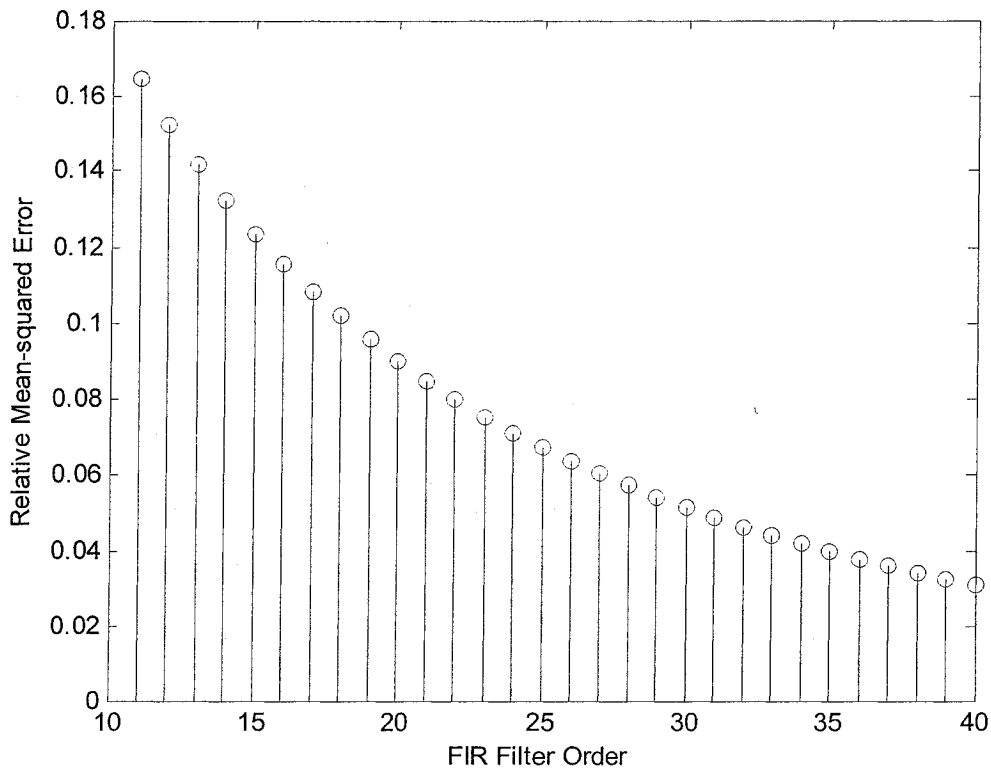

Figure 3-1: The relative mean-squared error between the exact magnitude response and the FIR approximation.

The magnitude response of some generated FIR filters is depicted in Figure 3-2:

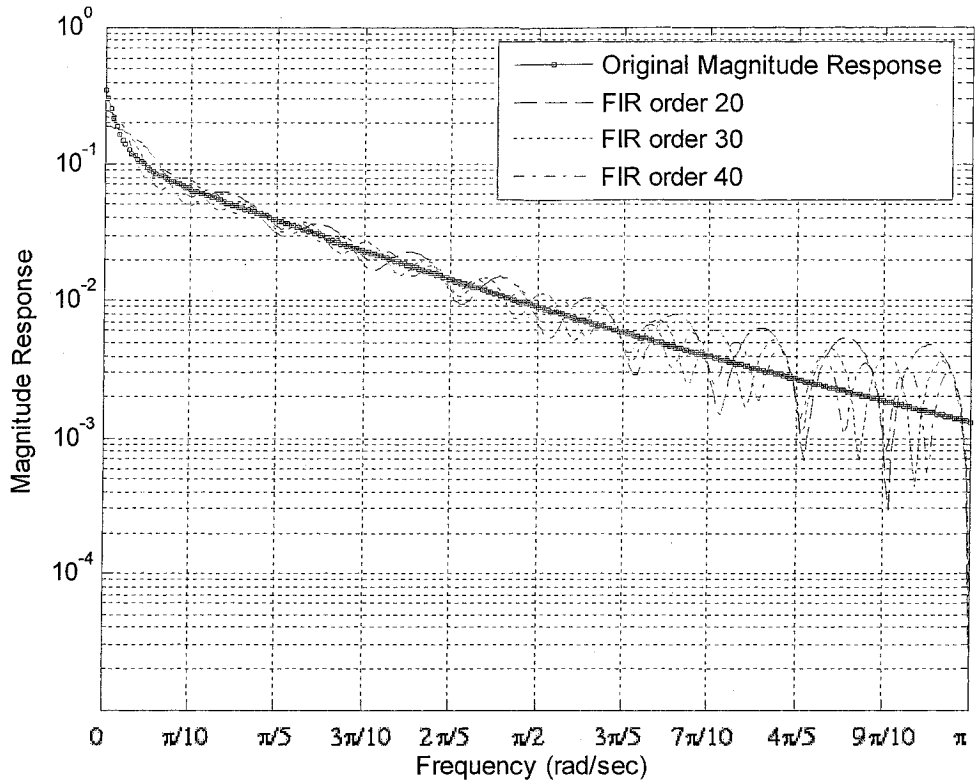

Figure 3-2: The original magnitude response and the magnitude response of some FIR filters.

As one may expect, the higher the order of the FIR filter is, the better the approximation is. However, one should also take the complexity of the filter into account when it comes to the filter approximation. The errors corresponding to different filter orders are given in Table 3-1. The coefficients of the 30^{th} order FIR filter generated using the above method are given in Table 3-2.

In presence of weighting function, the FIR filter approximation becomes more complicated but at the same time more effective in terms of approximating the output signal of a DSL line, if PSD of the corresponding DSL service is used as the weighting function.

Table 3-1: Approximation (mean-squared) error for typical order of FIR filters

FIR Filter O7rder	*Approximation Error*	*FIR Filter Order*	*Approximation Error*
15	1.5103e-4	20	1.0985e-4
25	8.2074e-5	30	6.2519e-5
35	4.8385e-5	40	3.7919e-5

Table 3-2: Coefficients of 30th order FIR filter

Coefficient Number	*FIR Filter Coefficients*				
1-5	0.0108	0.0190	0.0192	0.0165	0.0136
6-10	0.0114	0.0098	0.0087	0.0079	0.0073
11-15	0.0069	0.0066	0.0063	0.0060	0.0058
16-20	0.0056	0.0054	0.0052	0.0050	0.0049
21-25	0.0047	0.0046	0.0045	0.0043	0.0042
25-30	0.0041	0.0040	0.0039	0.0038	0.0036

The FIR filters are obtained by minimizing the weighted error for 30 different filter orders and the corresponding relative approximation errors are depicted in Figure 3-3. The resultant magnitude responses for four different orders are given in Figure 3-4 and the coefficients of the 30th order FIR filter are given in Table 3-3. The weighting function used here is a simplified version of the PSD of a typical ADSL service (a piecewise constant approximation, as shown in Figure 3-5). The figure shows the magnitude response of the DSL line configuration shown in Figure 2-5(a) and that of a FIR filter of order 40, obtained by minimizing the performance index (3.2) with the above mentioned weighting function. Note that the sharp jump of the magnitude response of the approximate model outside the nonzero region of the weighting function is due to

the fact that the value of the magnitude response in those intervals is not important. Since the weighting function here is considered to be the PSD of the DSL signal, this implies that the transmitted signal has no power in those frequency intervals.

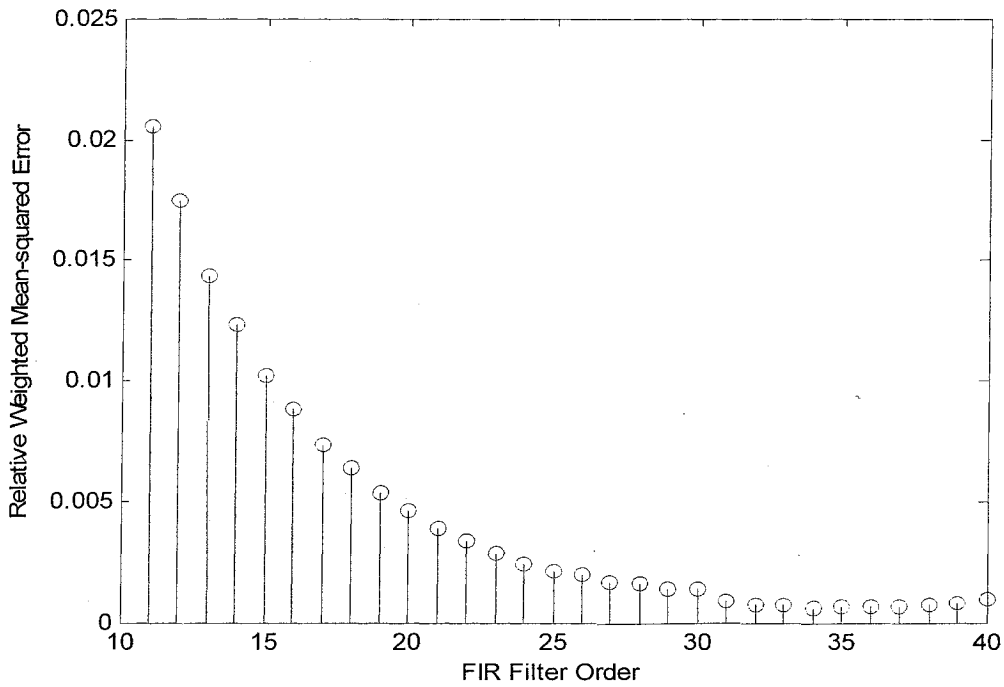

Figure 3-3: The relative weighted mean-squared error between the exact magnitude response and the FIR approximation.

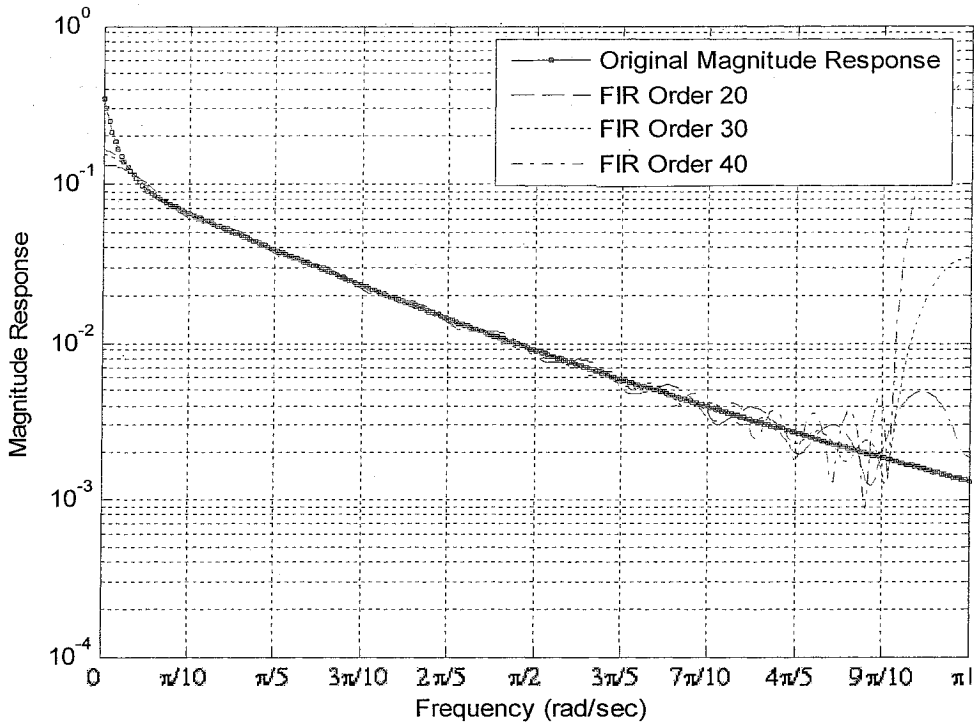

Figure 3-4: The original magnitude response and the magnitude response of some FIR filters processed using a weighting function.

Table 3-3: Coefficients of the 30th order FIR filter using weighting function

Coefficient Number	*FIR Filter Coefficients*				
1-5	0.0079	0.0185	0.0182	0.0164	0.0119
6-10	0.0107	0.0072	0.0078	0.0047	0.0064
11-15	0.0032	0.0057	0.0022	0.0052	0.0014
16-20	0.0047	0.0008	0.0042	0.0004	0.0037
21-25	0.0002	0.0032	0.0001	0.0026	0.0002
26-30	0.0020	0.0002	0.0014	0.0003	0.0010

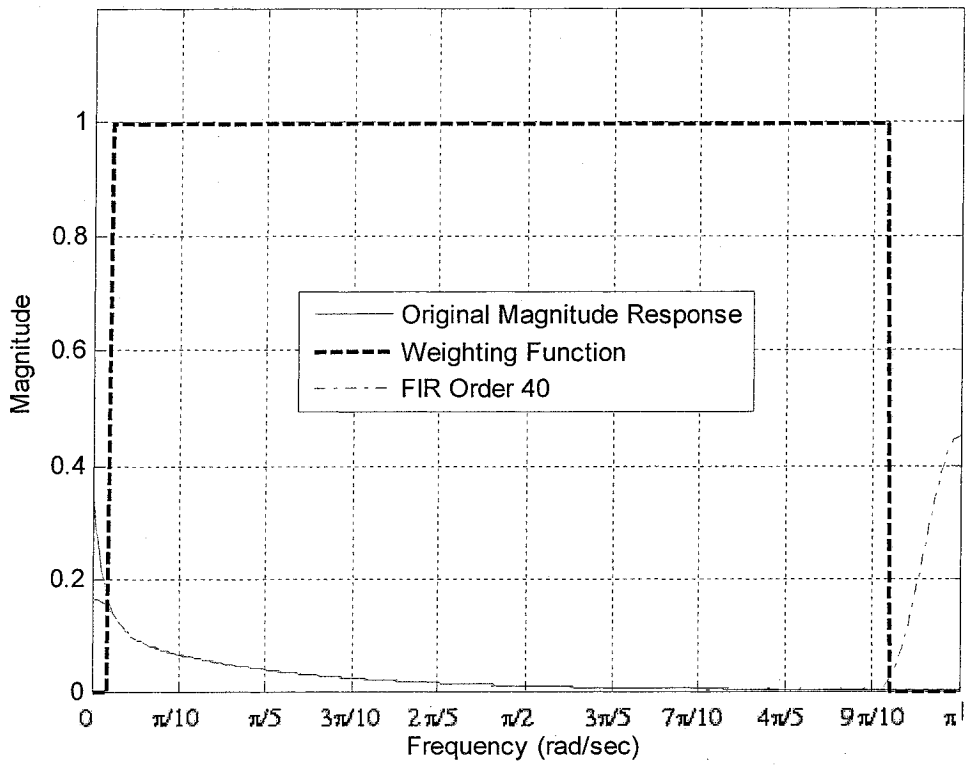

Figure 3-5: The original magnitude response and the magnitude response of a FIR filter with order 40 generated using the weighting function shown in the picture.

Chapter 4

4 Model Reduction

In this chapter, the techniques of reducing the order of digital filters are discussed. The model reduction techniques in control theory will be used to reduce the order of a discrete-time finite dimensional LTI filter.

The main objective of model order reduction problems is to find an approximate model for any given high-order system. It is desired to preserve stability in the reduced-order model. It is also desired to provide an upper bound for the norm of approximation error, which shows the accuracy of the result. Model order reduction techniques in control can be used to reduce the order of a digital filter as a discrete-time high-order system.

Balanced Truncation which truncates the states of the balanced realization [14-15] obtained from a proper similarity transformation, is an efficient method for model order reduction in control systems specially because it gives an upper bound for the error between the original and reduced order models.

4.1 State-space Realization

A finite dimensional continuous-time LTI system is described in the state-space form as:

$$\begin{aligned} \dot{x}(t) &= A_C x(t) + B_C u(t) \\ y(t) &= C_C x(t) + D_C u(t) \end{aligned} \tag{4.1}$$

and in discrete-time case:

$$\begin{aligned} x[n+1] &= Ax[n] + Bu[n] \\ y[n] &= Cx[n] + Du[n] \end{aligned} \tag{4.2}$$

where matrices A, B, C and D are state transition, input, output (measurement) and coupling matrices, respectively. In the simple case of Single-Input Single-Output (SISO) systems, B and C are vectors and D is a scalar.

For a system with distinct poles, the transfer function of a discrete-time system can be decomposed as:

$$H(z) = d + \sum_{i=1}^{k} \frac{c_i}{z - p_i} \tag{4.3}$$

Using this decomposition, the state-space realization of the system can be written in the following diagonalized form [29]:

$$
\begin{aligned}
A &= \begin{bmatrix} p_1 & 0 & \cdots & \cdots & 0 \\ 0 & p_2 & 0 & \cdots & 0 \\ \vdots & \ddots & \ddots & \ddots & \vdots \\ 0 & \cdots & 0 & p_{k-1} & 0 \\ 0 & \cdots & \cdots & 0 & p_k \end{bmatrix} \\
B &= \begin{bmatrix} 1 \\ 1 \\ \vdots \\ \vdots \\ 1 \end{bmatrix} \\
C &= \begin{bmatrix} c_1 & c_2 & \cdots & c_{k-1} & c_k \end{bmatrix} \\
D &= \begin{bmatrix} d \end{bmatrix}
\end{aligned}
\tag{4.4}
$$

Stability of the system can be verified by checking the location of the eigenvalues of the matrix A, because they are simply equal to the poles of the system. In general, the transfer function of a system is related to the state-space realization through the following equation:

$$H(z) = C(zI - A)^{-1}B + D \tag{4.5}$$

which in turns implies that the poles of the system are the roots of the equation given by setting the determinant of $(zI - A)$ to zero [22].

For a system (either discrete-time or continuous-time) with the numerator and denominator coefficients indicated by b_k's and a_k's, the state-space matrices will be given by:

$$
\begin{aligned}
A &= \begin{bmatrix} 0 & 1 & 0 & \cdots & 0 \\ 0 & 0 & 1 & \ddots & \vdots \\ \vdots & \vdots & 0 & \ddots & 0 \\ 0 & 0 & \cdots & 0 & 1 \\ -a_0 & -a_1 & -a_2 & \cdots & -a_{N-1} \end{bmatrix} \\
B &= \begin{bmatrix} 0 \\ 0 \\ \vdots \\ 0 \\ 1 \end{bmatrix} \\
C &= \begin{bmatrix} b_0 - b_N a_0 & b_1 - b_N a_1 & \cdots & b_{N-2} - b_N a_{N-2} & b_{N-1} - b_N a_{N-1} \end{bmatrix} \\
D &= \begin{bmatrix} b_N \end{bmatrix}
\end{aligned}
\tag{4.6}
$$

In the case of FIR filters, since the poles are all located in the origin, it is not possible to realize this kind of filters in state-space domain by diagonalization. However, one can obtain a canonical representation for the model, as follows:

$$
\begin{aligned}
A &= \begin{bmatrix} 0 & 1 & 0 & \cdots & 0 \\ 0 & 0 & 1 & \ddots & \vdots \\ \vdots & \vdots & 0 & \ddots & 0 \\ 0 & 0 & \cdots & 0 & 1 \\ 0 & 0 & 0 & \cdots & 0 \end{bmatrix} \\
B &= \begin{bmatrix} 0 \\ 0 \\ \vdots \\ 0 \\ 1 \end{bmatrix} \\
C &= \begin{bmatrix} b_0 & b_1 & \cdots & b_{N-2} & b_{N-1} - b_N \end{bmatrix} \\
D &= \begin{bmatrix} b_N \end{bmatrix}
\end{aligned}
\tag{4.7}
$$

4.2 Balanced Realization

A realization of a finite dimensional LTI system is said to be balanced if its controllability and observability gramians are equivalent and diagonal. Consider the system (4.2). If the system is asymptotically stable, then the controllability and observability gramians can be computed by solving the following Lyapunov equation [11-12]:

$$\begin{aligned} AW_C A' - W_C + BB' = 0 \\ A'W_O A - W_O + C'C = 0 \end{aligned} \tag{4.8}$$

For a continuous-time system given by (4.1), the Lyapunov equation will be as follows [3], [6]:

$$\begin{aligned} A_C W_C + W_C A_C' + B_C B_C' = 0 \\ A_C' W_O + W_O A_C + C_C' C_C = 0 \end{aligned} \tag{4.9}$$

Suppose that the state-space system becomes balanced using the following change of coordinates:

$$x[n] = Tz[n] \tag{4.10}$$

Then, the controllability and observability gramians of the original system and balanced system will be related through the following equations:

$$W_C = T\hat{W}_C T^T$$
$$W_O = T^{-T}\hat{W}_O T^{-1} \tag{4.11}$$

The same relations hold between the gramians for the continuous-time case. This results in:

$$\hat{W}_C\hat{W}_O = T^{-1}W_C T^{-T}T^T W_O T = T^{-1}W_C W_O T \tag{4.12}$$

The eigenvalues of $W_C W_O$ are equal to those of $T^{-1}W_C W_O T$, which are, in fact, equal to square of Hankel singular values of the gramians. In other words:

$$sp(W_C W_O) = sp(\hat{W}_C\hat{W}_O) = sp\left(\begin{bmatrix} \sigma_1 & 0 & \cdots & 0 \\ 0 & \sigma_2 & \ddots & \vdots \\ \vdots & \ddots & \ddots & 0 \\ 0 & \cdots & 0 & \sigma_N \end{bmatrix}\begin{bmatrix} \sigma_1 & 0 & \cdots & 0 \\ 0 & \sigma_2 & \ddots & \vdots \\ \vdots & \ddots & \ddots & 0 \\ 0 & \cdots & 0 & \sigma_N \end{bmatrix}\right) \tag{4.13}$$
$$= \left\{\sigma_1^2, \sigma_2^2, \cdots, \sigma_N^2\right\}$$

where $sp(\cdot)$ represents eigenvalues of a matrix. The same efficient numerical solution for the Lyapunov equation has been studied by several researchers, e.g. see [23-24]. When the system is balanced, the HSVs in (4.13) are in descending order. Therefore in balanced truncation, the states with smaller HSVs are eliminated. This means that the states that are less observable and controllable in the balanced realization will have no effect in the reduced-order model. Sometimes a constant gain is multiplied by the transfer function of

the reduced-order model to make the DC-gain of the resultant model equal to that of the original model. DC gain adjustment is very advantageous in tracking problems. Balanced truncation provides an error bound based on HSVs of the original system [9], [15]:

$$\left\| H - \hat{H} \right\|_{\infty} \leq 2\left(\sigma_{k+1} + \cdots + \sigma_{N}\right) \tag{4.14}$$

where $\|\cdot\|_{\infty}$ denotes the infinity norm or the largest magnitude of the frequency response of the model error. This equation shows that the magnitude of the error depends on the tail of HSVs of the system, meaning that the error bound depends on the magnitude of the HSVs associated with the eliminated states in the balanced realization. This also implies that the error depends on the value of the order of reduced order model (k), which in turn indicates the starting point of the 'tail' [34].

Some works have been done on how to choose the truncation point, but in general, it is a design parameter which depends on the desired accuracy. The simplest method for choosing the truncation point is based on the difference of adjacent HSVs. In other words, the truncation point where the absolute value of difference reaches its maximum, or alternatively, where HSVs begin to decrease sharply.

Another truncation method is to observe the ratio of adjacent HSVs, and truncate the series when the σ_k / σ_{k+1} ratio is sufficiently large [1].

4.2.1 Balanced Realization For FIR Filters

In case of FIR filters, it can be shown that the controllability and observability gramians of the discrete-time system have special forms. Suppose that the FIR filter is given by:

$$y[n] = b_0 x[n] + b_1 x[n-1] + \cdots + b_N x[n-N] \tag{4.15}$$

The state-space model can be represented by the following matrices:

$$\begin{aligned} A &= \begin{bmatrix} 0 & 1 & 0 & \cdots & 0 \\ 0 & 0 & 1 & \cdots & 0 \\ \vdots & \vdots & \vdots & \ddots & \vdots \\ 0 & 0 & 0 & \cdots & 1 \\ 0 & 0 & 0 & \cdots & 0 \end{bmatrix} \\ B &= \begin{bmatrix} 0 \\ 0 \\ \vdots \\ 0 \\ 1 \end{bmatrix} \\ C &= \begin{bmatrix} b_N & b_{N-1} & \cdots & b_2 & b_1 \end{bmatrix} \\ D &= \begin{bmatrix} b_0 \end{bmatrix} \end{aligned} \tag{4.16}$$

It can be shown that for this state-space model, the controllability gramian will be equal to the identity matrix, i.e.

$$W_C = I_{N\times N} \tag{4.17}$$

and the observability gramian will be equal to:

$$W_O = \begin{bmatrix} b_N^2 & b_N b_{N-1} & \cdots & b_N b_2 & b_N b_1 \\ b_N b_{N-1} & b_N^2 + b_{N-1}^2 & \cdots & b_N b_3 + b_{N-1} b_2 & b_N b_2 + b_{N-1} b_1 \\ \vdots & \vdots & \ddots & \vdots & \vdots \\ b_N b_2 & b_N b_3 + b_{N-1} b_2 & \cdots & b_N^2 + b_{N-1}^2 + \cdots + b_2^2 & b_N b_{N-1} + b_{N-1} b_{N-2} + \cdots + b_2 b_1 \\ b_N b_1 & b_N b_2 + b_{N-1} b_1 & \cdots & b_N b_{N-1} + b_{N-1} b_{N-2} + \cdots + b_2 b_1 & b_N^2 + b_{N-1}^2 + \cdots + b_1^2 \end{bmatrix} \tag{4.18}$$

The observability gramian itself can be written as a multiplication of an upper-diagonal and a lower-diagonal matrix as follows:

$$W_O = XX^T$$

where:

$$X = \begin{bmatrix} b_N & 0 & \cdots & 0 & 0 \\ b_{N-1} & b_N & \cdots & 0 & 0 \\ \vdots & \vdots & \ddots & \vdots & \vdots \\ b_2 & b_3 & \cdots & b_N & 0 \\ b_1 & b_2 & \cdots & b_{N-1} & b_N \end{bmatrix} \tag{4.19}$$

It is to be noted that the entries of the matrix X are the coefficients of the FIR filter. Using the properties of gramians of the system before and after applying balanced realization, one concludes that:

$$sp(W_I W_O) = sp(W_O) = sp(XX^T) = \{\sigma_1^2, \sigma_2^2, \cdots, \sigma_N^2\} \tag{4.20}$$

On the other hand:

$$\sigma(X) = \sqrt{sp(X^T X)} \tag{4.21}$$

Thus:

$$\sigma(X) = \{\sigma_1, \sigma_2, \cdots, \sigma_N\} \tag{4.22}$$

This implies that the singular values of the triangular matrix X are equal to the HSVs of the system. Thus, one can find the HSVs of a system representing a FIR filter without directly applying balanced realization technique by simply calculating the singular values of a matrix which consists of the coefficients of the FIR filter.

Example 4.1: In this example, balanced realization is used to reduce the order of a discrete-time finite-dimensional LTI filter. The filter is 30^{th} order low-pass IIR filter. The zero-pole map of the filter is shown in Figure 4-1. This IIR filter represents the magnitude response of the DSL configuration shown in Figure 2-5(b).

After applying balanced realization to the above mentioned filter, the HSVs of the system are arranged in descending order as shown in Figure 4-2. The order reduction process begins with removing the states with larger HSVs, i.e. the first states of the system. The more the states are removed, the bigger the error between the original and reduced-order system will be. The infinity-norm of the error between the 30^{th} order low-pass IIR filter and the reduced-order system is depicted in Figure 4-3.

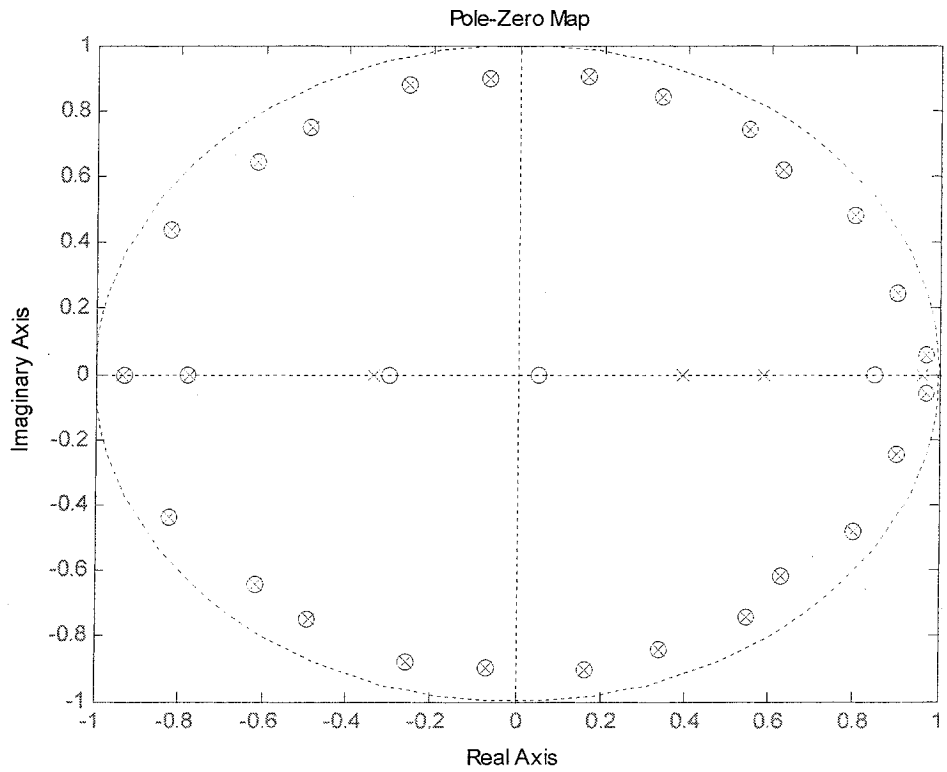

Figure 4-1: Zero-pole map of the filter

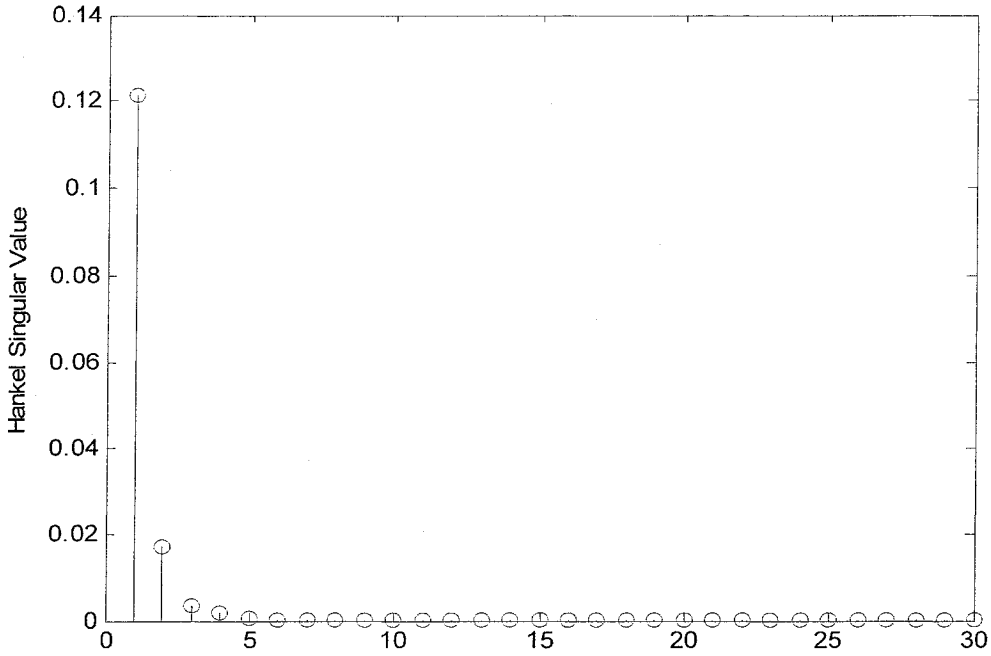

Figure 4-2: Hankel singular values shown in descending order

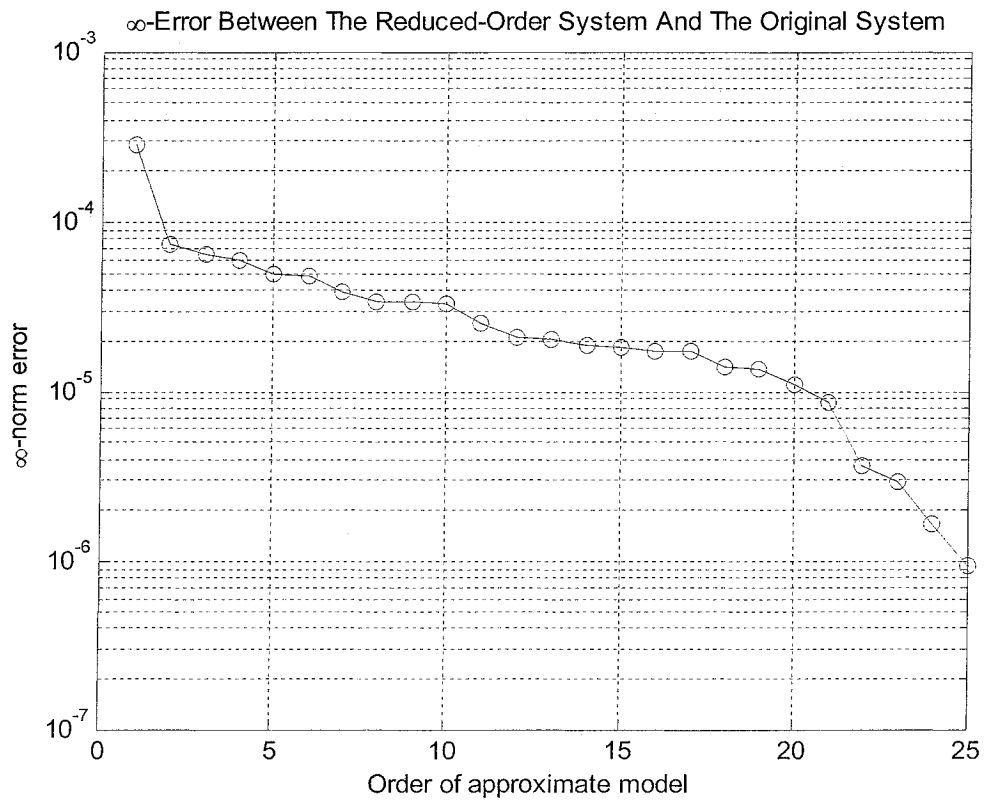

Figure 4-3: ∞-Error between the reduced-order system and the original system

4.3 IIR-FIR-IIR Approach in Model Order Reduction

A new method will now be proposed to approximate an IIR filter using a reduced-order IIR model. This will be referred to as IIR-FIR-IIR approach, in which the IIR filter is once approximated by a FIR filter and again by an IIR filter [2], [4]. It is to be noted that as discussed in section 4.2.1, controllability and observability gramians of a FIR filter can be written in a closed form in terms of the filter coefficients. This is, in fact, the main motivation of the proposed algorithm. The resultant IIR filter has an order less than the order of the original one and its accuracy can be improved through iterations as will be discussed later.

A similar process is used in system identification where a hybrid adaptive FIR/IIR filter configuration is considered. The process consists of finding an adaptive FIR filter by applying a training signal in order to find a near optimum approximation, mapping the FIR filter coefficients through a model reduction technique to a smaller set of coefficients for initializing an adaptive IIR filter and finally fine tuning the IIR filter for more accuracy [30-32].

An IIR filter can be approximated by a FIR model using long division. It is obvious that a FIR model with more terms obtained by truncating the long division will result in smaller error between the original IIR filter and its FIR counterpart. The error can be measured in terms of 2-norm, ∞-norm, or any other performance index given as a design specification. A finite-dimensional LTI discrete-time causal filter can be represented as (3.5), where $a_N = 1$. The long division process gives a FIR filter whose

coefficients are obtained directly from the coefficients of the numerator and denominator of the IIR filter. The coefficients of a FIR filter obtained from long division can be computed as:

$$c_k = \begin{cases} b_k - \sum_{l=1}^{k} c_{k-l} a_l & k \le N \\ -\sum_{l=1}^{N} c_{k-l} a_l & k > N \end{cases} \tag{4.23}$$

which turns out to be a recursive equation. It can be concluded from equation (4.23) that the coefficients of the FIR filter can be generated from the coefficients of the numerator and denominator of the IIR filter and at most N recently generated coefficients of the FIR filter. The recursion can continue to obtain a truncated FIR filter of any arbitrary order, typically greater than N. More specifically, the recursion can continue until the error between the resultant FIR filter and the original IIR filter is sufficiently small.

It should be noted that since the coefficients of the filter obtained from long division represent the samples of the impulse response, the stability of the filter requires that the samples converge to zero. This follows immediately from the fact that a discrete-time LTI system is stable if and only if the impulse response of the system is absolutely summable [28]. This implies that the coefficients of the resultant FIR filter are expected to approach zero as time increases.

Truncation of the series of coefficients generated by long division gives a FIR filter with order N which is equal to the number of coefficients preserved after the truncation. In general, as the number of terms in the resultant FIR filter increases, it gives a better approximation for the original IIR filter.

The resultant FIR model will then be transformed using balanced realization and its order will be reduced using the method discussed in section 4.2.1. The resultant model will be an IIR filter. An upper bound on the infinity-norm of the error between the original and reduced order IIR filters, $H_{IIR}(z)$ and $\widetilde{H}_{IIR}(z)$, can be obtained by using the following inequality [22]:

$$\left\|H_{IIR}(z)-\widetilde{H}_{IIR}(z)\right\|_{\infty} \le \left\|H_{IIR}(z)-H_{FIR}(z)\right\|_{\infty} + \left\|H_{FIR}(z)-\widetilde{H}_{IIR}(z)\right\|_{\infty} \tag{4.24}$$

in which $H_{FIR}(z)$ represents the intermediate FIR filter. Note that the first term in the right side of the above inequality is the error due to the truncation in the long division used to obtain the FIR filter from the original IIR filter, and the second term is the error due to the model order reduction using balanced realization technique. Note also that a bound on the error introduced by model order reduction is given by (4.14).

In case of an unstable IIR filter, the transfer function $H_{IIR}(z)$ can be decomposed into the product of two transfer functions $H_{IIR}(z)=H_1(z)H_2(z)$, where $H_1(z)$ contains all stable poles and $H_2(z)$ contains all unstable poles. The model-order reduction can then be performed only on $H_1(z)$ to obtain $\widetilde{H}_1(z)$. The result can finally be multiplied by $H_2(z)$ to obtain the reduced-order transfer function for the original IIR system, i.e. $\widetilde{H}_{IIR}(z)=\widetilde{H}_1(z)H_2(z)$. Also for an IIR system with a nonzero D in the state-space model, one can define a new transfer function $H_1(z)=H_{IIR}(z)-D$ (note that for a scalar transfer function D will be scalar). Then, the balanced realization method can be applied

to $H_1(z)$ to find $\widetilde{H}_1(z)$. D can then be added to $\widetilde{H}_1(z)$ to obtain the desired reduced-order transfer function for the original system, i.e. $\widetilde{H}_{IIR}(z) = \widetilde{H}_1(z) + D$.

An algorithm can be proposed here in order to perform the model order reduction based on the above theoretical notes. Consider an IIR filter of order N whose transfer function is given by (3.5). It is desired to approximate this filter with another IIR filter of order M, $M<N$. Use (3.5) to find the first $N+1$ coefficients $c_0, c_1, \ldots, c_N$ of the FIR filter resulting from long division and truncation applied to the IIR filter. Set the variable k equal to $N+1$ and apply the following procedure:

Algorithm 4.1:

(i) Use the coefficients $c_0, c_1, \ldots, c_k$ to create a new FIR filter of order k. Note that this filter is obtained by applying long division and truncation to the given IIR filter transfer function as described in (3.5).

(ii) Evaluate the infinity-norm of the truncation error resulted in the previous step, and denote it by $e_{1,k}$.

(iii) Form the matrix X as described in (4.19), using the coefficients of the FIR filter obtained in step (i). Find the singular values of X.

(iv) Evaluate the order reduction error bound, $e_{2,k}$, using k-M+1 smallest singular values as given in (4.14). If $k=N+1$, go to step (i).

(v) Check if $e_k = e_{1,k} + e_{2,k}$ is a sufficiently small error bound. If not, increase k by one and go to step (i).

(vi) Balance the FIR filter using balanced realization technique and remove the last k-M+1 states. The reduced order IIR model is composed of the remaining modes.

It is to be noted that Algorithm 4.1 starts with k=N+1, as a FIR filter of order less than N+1 obtained by applying long division and truncation to an IIR system will, in general, have a large error associated with it. Thus, it will not be sufficiently close to the IIR system, which means that it will not be a good candidate to start the algorithm.

Also for a given value of M as the desired order, the approximation error using any model-order reduction technique is not negligible. In other words, the error bound obtained in step (v) cannot be arbitrarily small even if $k \rightarrow \infty$. This means that one should consider a reasonable error bound to compare with e_k in step (v). In general, one should stop increasing k in Algorithm 4.1 when e_k reaches a steady value with respect to k. At that point, $e_{1,k}$ is sufficiently smaller than $e_{2,k}$, which implies that the overall error bound is approximately equal to $e_{2,k}$.

The reduced-order model resulted by using the proposed algorithm has a DC-gain equal to that of the original system. In many practical applications, ω=0 is the most important frequency and having equal DC-gains is desirable. However, in some applications such as band-pass filters, it is desired to have equal magnitude responses at a nonzero frequency. This can be accomplished by multiplying the transfer function of the resultant reduced-order model by a constant coefficient.

Example 4.2: Consider again the IIR filter of order 30 whose zero-pole configuration is shown in Figure 4-1. The numerator and denominator coefficients of this filter are given in Table 4-1:

Table 4-1: Coefficients of the 30th order IIR filter

Coefficient Number	***Numerator Coefficients***				
1-5	0	0.0187	-0.0566	0.0811	-0.0816
6-10	0.0670	-0.0485	0.0313	-0.0163	0.0044
11-15	0.0052	-0.0123	0.0173	-0.0202	0.0221
16-20	-0.0254	0.0299	-0.0310	0.0272	-0.0204
21-25	0.0123	-0.0053	-0.0002	0.0041	-0.0064
26-30	0.0071	-0.0056	0.0026	-0.0001	-0.0004
31	0.0000				
Coefficient Number	***Denominator Coefficients***				
1-5	1.0000	-4.0365	7.5547	-9.2123	8.6181
6-10	-6.7989	4.7364	-2.8452	1.2650	-0.0026
11-15	-0.9745	1.6829	-2.1471	2.4311	-2.7209
16-20	3.1473	-3.4718	3.3593	-2.7903	1.9504
21-25	-1.0840	0.3537	0.2019	-0.5694	0.7502
26-30	-0.7201	0.4839	-0.1735	-0.0114	0.0304
31	-0.0065				

It is desired to approximate the system with an IIR model of order 7. The FIR filter order k in step (i) of Algorithm 4.1 in this case will vary between 31 and 300. For each value of k, the infinity-norm of the error bound and the actual error are calculated and shown in Figure 4-4 [5]. The horizontal axis in this figure represents the order of the FIR filter (k in the algorithm). The vertical axis represents the infinity-norm of the error bound and actual error between the original IIR system and the reduced-order model in dB. As it can be seen from Figure 4-4, using a FIR filter of order 50 (k=50) as the intermediate filter for order reduction would result in a reasonably small error. It can be

verified that for k>50, the error resulted from Algorithm 4.1 is approximately equal to the error obtained by direct order reduction from the original IIR system to an IIR model of order 7, using balanced realization technique. However, unlike the direct order reduction, the proposed technique gives a closed form for the gramians which are required in balanced realization technique.

For comparison, the frequency response of the original IIR system and its 7^{th} order approximations obtained by using the proposed algorithm with k=50 and also, by applying model order reduction directly to the original IIR system using balanced realization technique, are shown in Figure 4-5. It can be seen from this figure that the result obtained by using Algorithm 4.1 is very close to the one obtained by direct order reduction which requires extensive numerical computations.

It is to be noted that the horizontal axis in Figure 4-4 takes integer values only as it represents FIR filter order. However, since the numbers on horizontal axis are very close, the resultant curves look like continuous graphs.

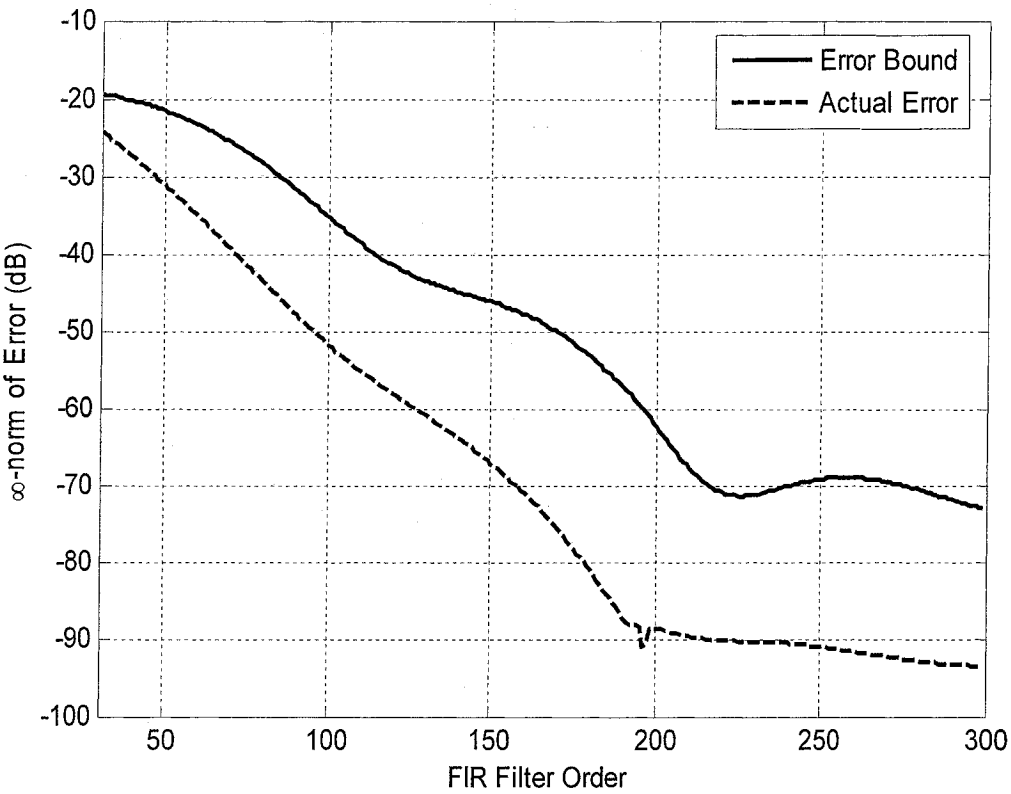

Figure 4-4: The estimated bound and exact value for infinity-norm of error in Example 4.2. The Horizontal axis shows the order of intermediate FIR filter using which the reduced order IIR filter is generated.

4.4 DSL Test Loops

In this section a set of standard test loops are used to verify the performance of the proposed algorithm. The ITU-T Recommendation G.996.1 describes the testing

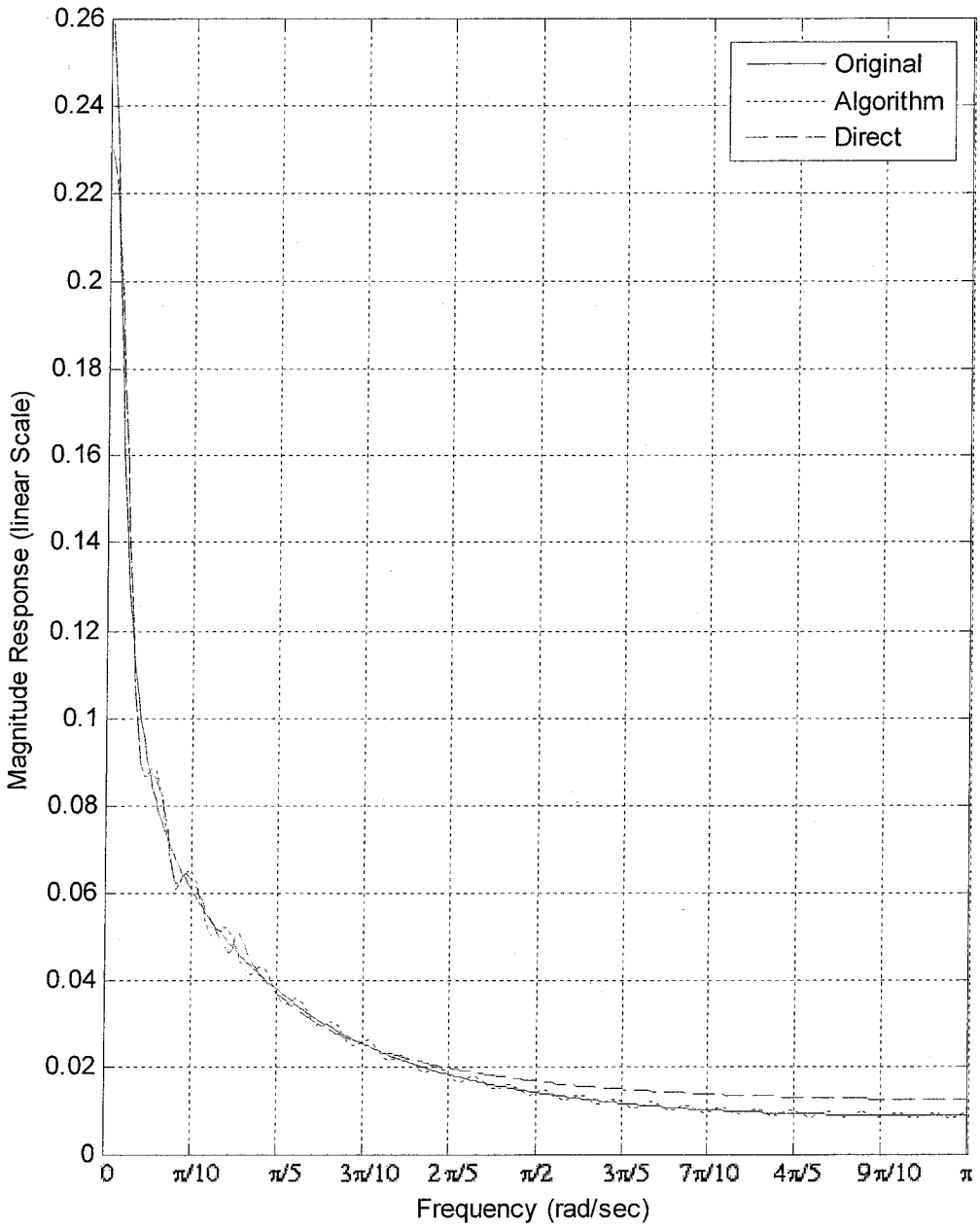

Figure 4-5: The magnitude responses of the original IIR system of Example 4.2, 7^{th} order approximation using the proposed algorithm with k=50, and 7^{th} order approximation applying balanced realization technique directly on the original system.

procedures for ITU Digital Subscriber Line (DSL) Recommendation [19-21]. This recommendation proposes some test loops and in-home wiring models which are specified for different regions of the world to test the DSL service performance.

The test loops are shown in Figure 4-6 with and without bridge taps, and also with different American Wire Gauges. The magnitude response of the test loops are shown in Figures 4-7 to 4-9. The frequency range for which the magnitude response is obtained is 0-1.2 MHz (which is the frequency range of the ADSL signal).

Since the transmission line is a continuous-time system, a continuous to discrete conversion should be used here. For each test loop it is assumed that a 30^{th} order continuous-time domain finite-dimensional LTI filter is available, and it is desired to have a 10^{th} order discrete-time filter. One can use two different approaches here: (i) apply balanced realization method to reduce the order of the continuous-time system, followed by Bilinear transformation to obtain the discrete-time equivalent model, and (ii) use Bilinear transformation to find the discrete-time equivalent model for the original continuous-time system and then apply model reduction through balanced realization for the discrete-time model. These two possible approaches are illustrated in Figure 4-10. The continuous-time domain LTI filters are actually generated by using the T-matrix modeling of Figure 2-3 and applying the modified Yule-Walker method [13]. The infinity-norm of error between the magnitude responses of the original system and the corresponding reduced-order model for each test loop is obtained using both approaches and the results are shown in Table 4-2.

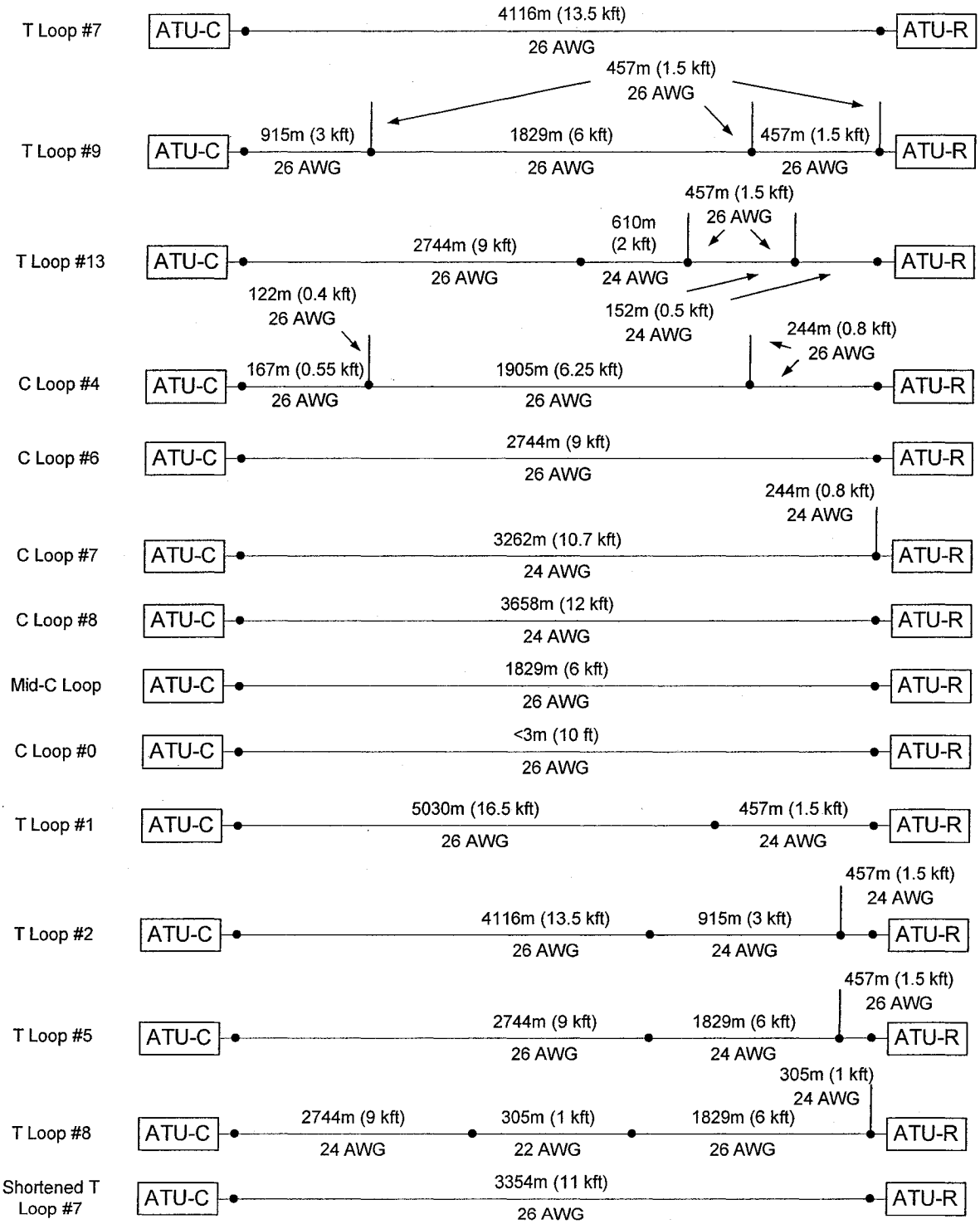

Figure 4-6: G.996.1 – North American test loops

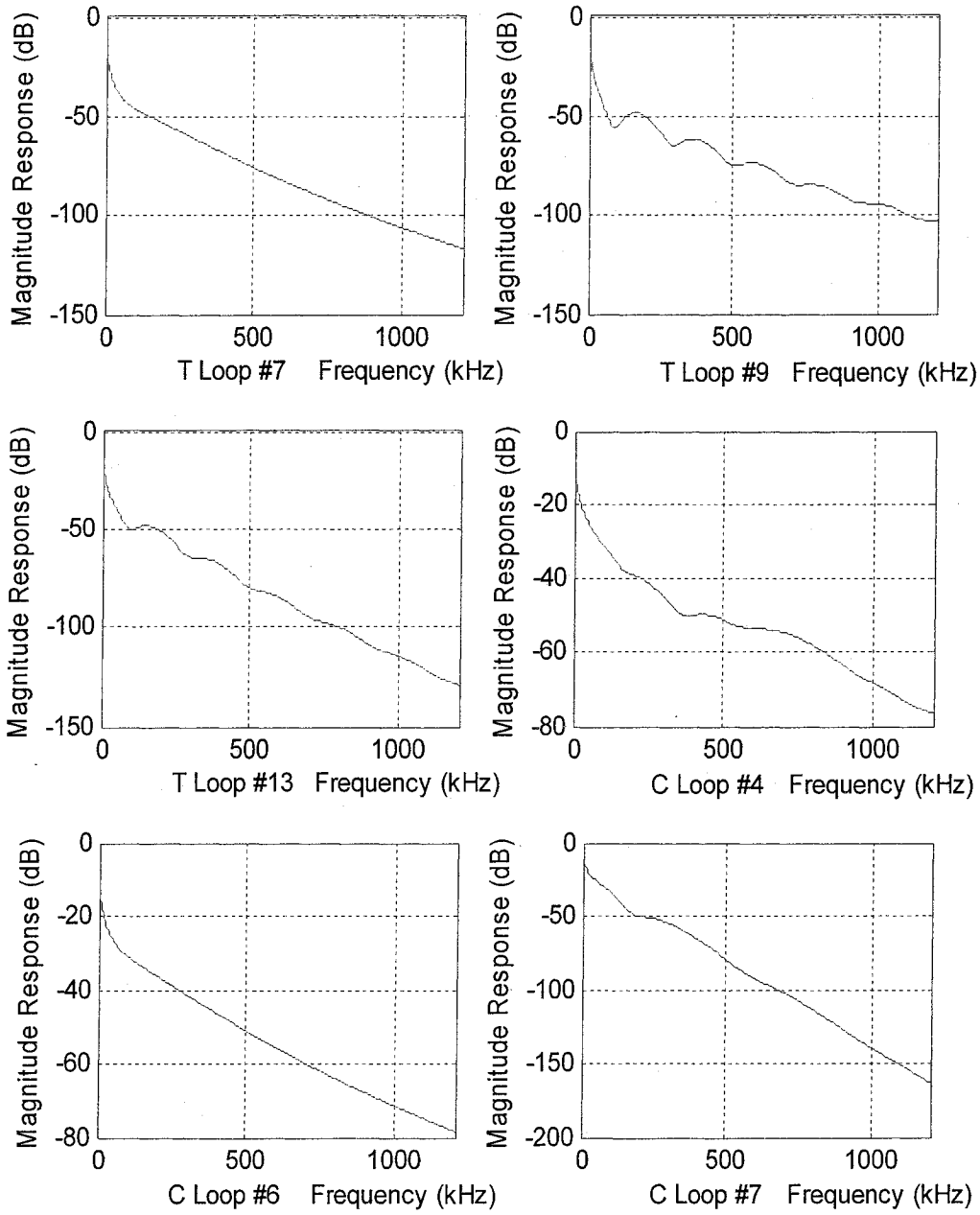

Figure 4-7: Magnitude response of T Loop #7, #9 and #13 and C Loop #4, #6 and #7

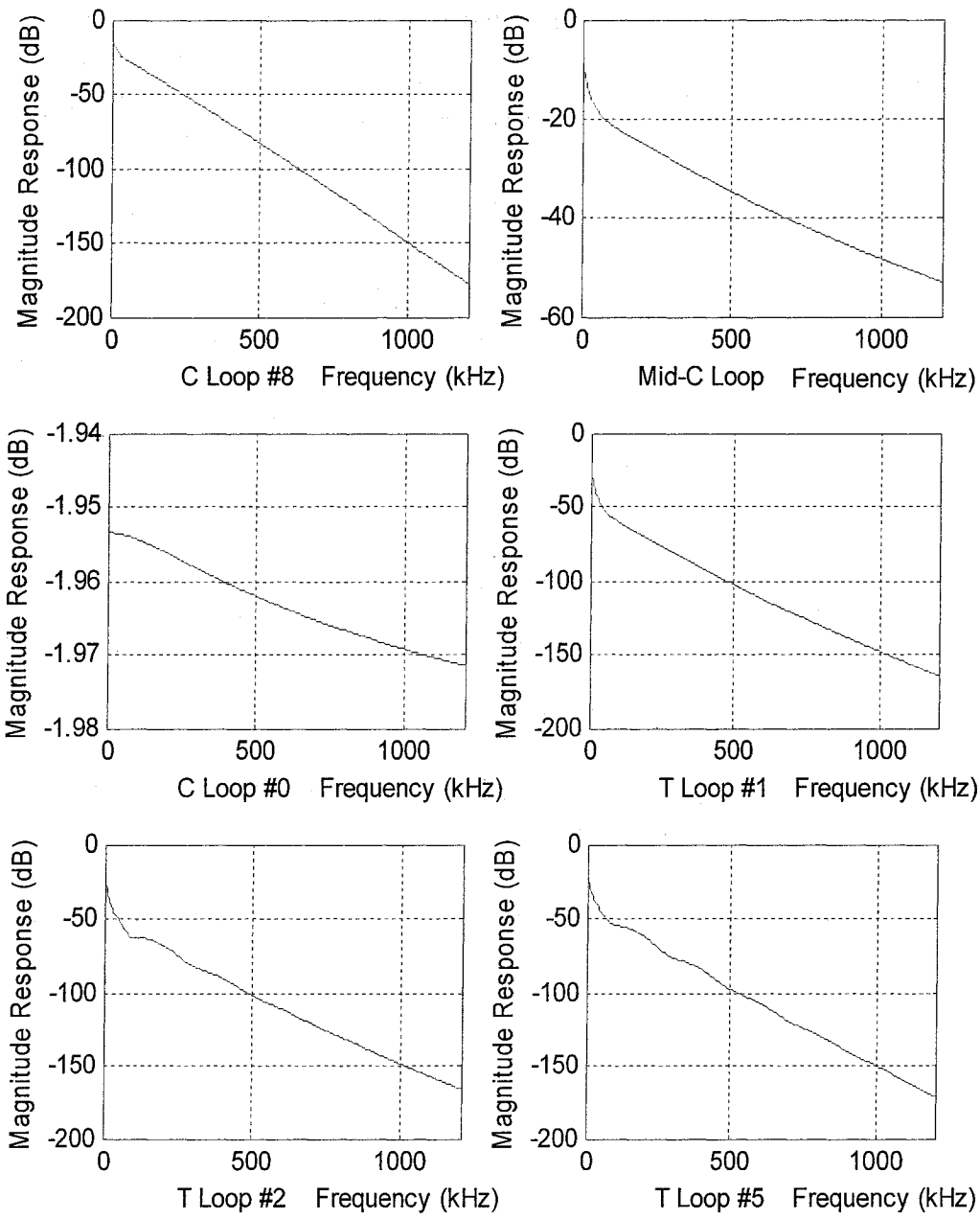

Figure 4-8: Magnitude response of C Loop #0 and #8, Mid-C Loop and T Loop #1, #2 and #5

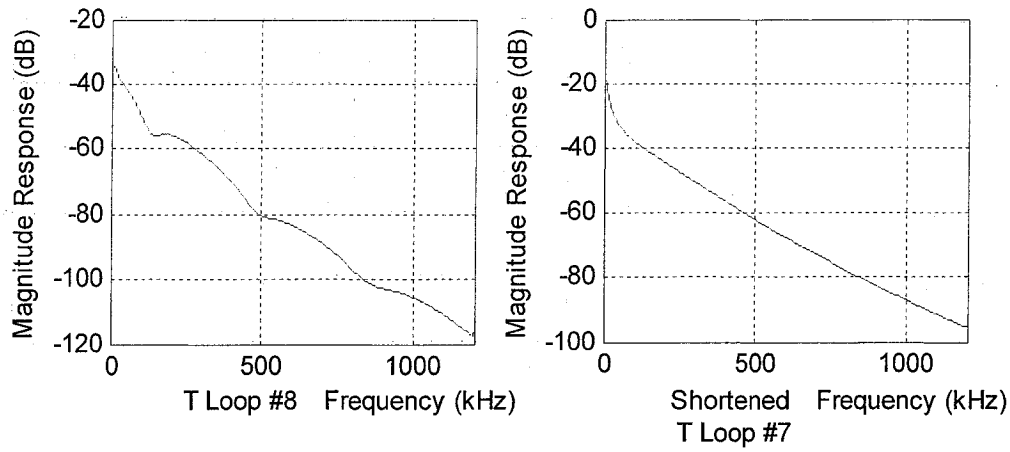

Figure 4-9: Magnitude response of T Loop #7 and #8

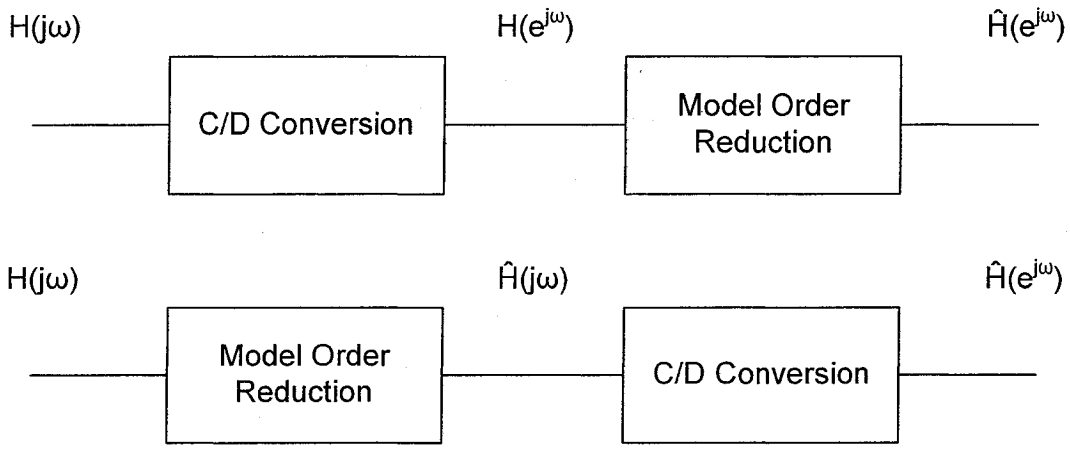

Figure 4-10: The two possible configurations: conversion-reduction and reduction-conversion

As can be seen in Table 4-2, for majority of test loops the two infinity-norm errors are more or less the same. For more observation, the above test is performed to generate models of different orders, meaning that the final order of the models vary from 1 to 29

as all original models are assumed to be 30^{th} order. The infinity-norm errors for each test loop and for all different orders are depicted in Figures 4-11 to 4-13.

Table 4-2: Infinity-norm error for all test loops using two different approaches of Figure 4-10

Test Loop	*Reduction-Conversion (dB)*	*Conversion-Reduction (dB)*
T Loop #7	-94.93	-94.93
T Loop #9	-77.57	-77.57
T Loop #13	-86.76	-86.76
C Loop #4	-69.33	-69.33
C Loop #6	-90.16	-90.16
C Loop #7	-68.52	-68.05
C Loop #8	-72.03	-72.57
Mid-C Loop	-86.48	-86.48
C Loop #0	-148.42	-148.42
T Loop #1	-87.17	-87.16
T Loop #2	-98.29	-93.36
T Loop #5	-83.12	-83.15
T Loop #8	-74.58	-74.58
Short T Loop #7	-102.88	-102.88

From these figures, one can find some infinity-norm error bounds for the reduced-order models of standard DSL test loops. For each loop, the reduced filter orders at which the infinity-norm error magnitudes reach certain levels are tabulated in Table 4-3.

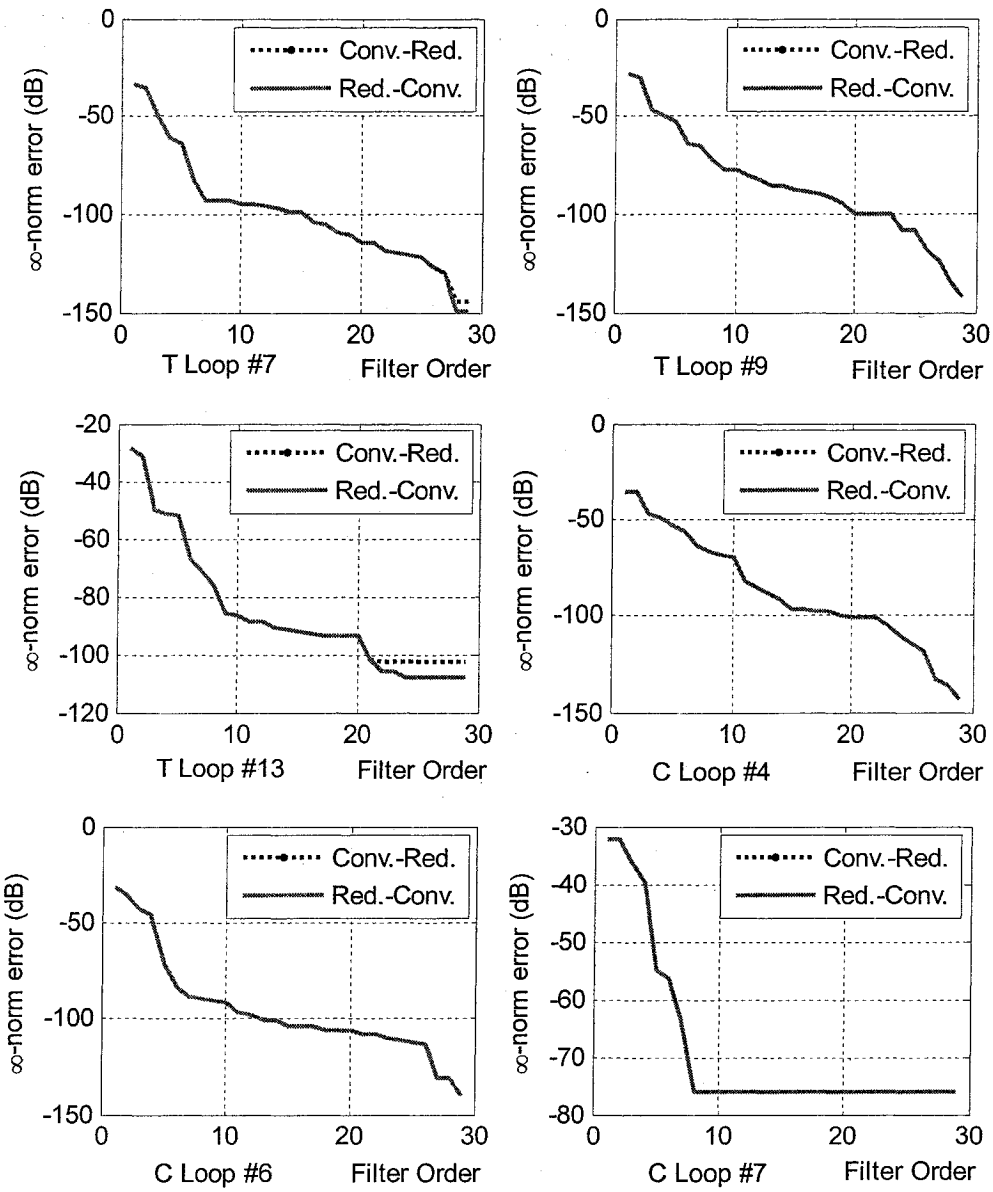

Figure 4-11: Infinity-norm error bounds for T Loop #7, #9 and #13 and C Loop #4, #6 and #7

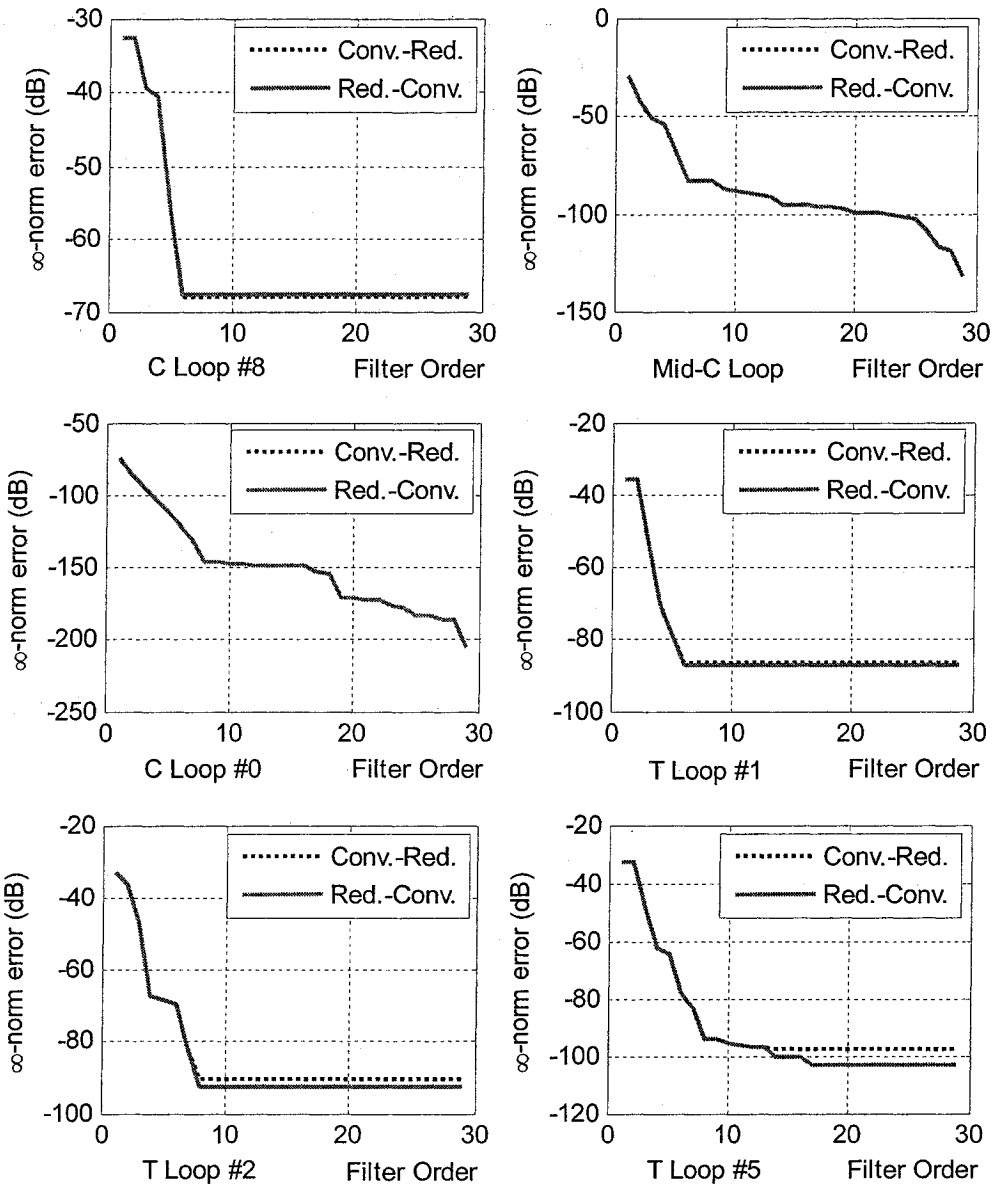

Figure 4-12: Infinity-norm error bounds for C Loop #0 and #8, Mid-C Loop and T Loop #1, #2 and #5

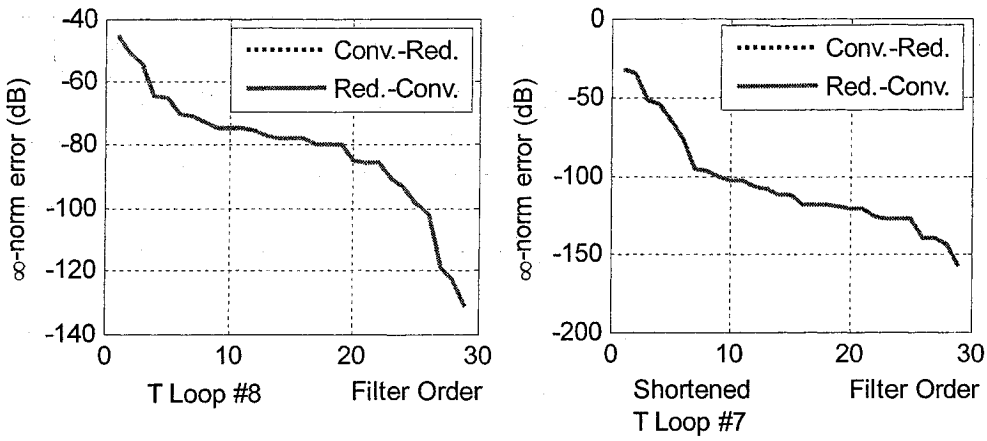

Figure 4-13: Infinity-norm error bounds for T Loop #7 and #8

Table 4-3: Suggested filter orders for specific error ranges

Test Loop	*Error Range*								
	10^{-2}	10^{-3}	10^{-4}	10^{-5}	10^{-6}	10^{-7}	10^{-8}	10^{-9}	10^{-10}
	Filter Order								
T Loop #7	3	4	6	16	24	28			
T Loop #9	3	6	11	20	27	29			
T Loop #13	3	6	9	21					
C Loop #4	3	7	11	19	27	29			
C Loop #6	3	5	6	13	27				
C Loop #7	5	7							
C Loop #8	3	6							
Mid-C Loop	2	5	6	20	29				
C Loop #0	1	1	2	4	6	8	19	25	29
T Loop #1	3	4	6						
T Loop #2	3	4	7						
T Loop #5	3	4	7	10					
T Loop #8	1	4	20	26	28				
Short T L #7	3	5	7	9	19	26			

Table 4-3 gives some information about the relation between the configuration of the test loops and their approximation results. The error magnitude for test loops C Loop #7 and #8 and also T Loop #1 and #2 does not become smaller than -80dB and their

magnitude response varies between -20dB and -160dB in the given range of frequency. In the real world, most loops are relatively long, with at most one bridge tap located at the end of the line which imposes very little impact on the magnitude response. This justifies why the infinity-norm of approximation error remains intact for some model orders. A non-monotonic magnitude response makes the approximate model less accurate. This implies that in the state-space representations, many states have a very small impact on the general behavior of the system. That is why in some cases even with removal of 20 states, changes in approximation error are negligible.

C Loop #0 is a special case since the magnitude varies only about 0.02dB. So the filter approximation will be more straightforward and the error magnitude will be smaller too. As it is shown in the table, the error reaches as low as -200dB which means that with relatively higher filter orders the error magnitude can potentially become much smaller.

T Loop #7 and #9 have more or less the same error performance. The magnitude response of T Loop #9 has more oscillations compared to T Loop #7 which is due to the existence of the three bridge taps. The magnitude varies between -20dB and -110dB within the given frequency range in both loops, but the oscillations (thence, more complexity) in the magnitude response of T Loop #9 leads to slightly higher filter order required for any desired error bound.

Another way of approximation of a filter is using a direct search optimization algorithm. The search method used here is Nelder-Mead simplex method which is available on MATLAB™ [25]. Reduction of 30^{th} order filter to a 10^{th} order model is done for all test loops and the coefficients of the resultant IIR filter are found using the above mentioned direct search method to minimize the infinity-norm error. The optimization

program is used with a weighting function equal to the ADSL PSD of Figure 2-8. Like any optimization procedure, Nelder-Mead's method requires initial point to start with. In this work, the initial point for each case is set to be the filter obtained using modified Yule-Walker method. The results are shown in Table 4-4:

Table 4-4: Infinity-norm error for all test loops using Nelder-Mead method

Test Loop	***Approximation Error***					
	Normal Search	dB	Weighted Search	dB	Balanced Realization	dB
T Loop #7	1.7934e-5	-94.93	1.7926e-5	-94.93	1.7921e-5	-94.93
T Loop #9	1.313e-4	-77.63	1.091e-4	-79.24	1.3235e-4	-77.57
T Loop #13	4.5942e-5	-86.76	4.4988e-5	-86.94	4.5925e-5	-86.76
C Loop #4	3.3856e-4	-69.41	2.96e-4	-70.57	3.4148e-4	-69.33
C Loop #6	3.0356e-5	-90.36	2.6209e-5	-91.63	3.1045e-5	-90.16
C Loop #7	3.6962e-5	-88.64	3.6907e-5	-88.66	5.1964e-5	-85.69
C Loop #8	2.487e-5	-92.09	2.4151e-5	-92.34	2.5027e-4	-72.03
Mid-C Loop	2.5912e-5	-91.73	2.5815e-5	-91.76	4.742e-5	-86.48
C Loop #0	3.7591e-8	-148.5	2.9916e-8	-150.5	3.7948e-8	-148.4
T Loop #1	2.1265e-6	-113.5	2.1172e-6	-113.5	4.3874e-5	-87.16
T Loop #2	1.6737e-5	-95.53	1.6736e-5	-95.53	2.149e-5	-93.36
T Loop #5	9.7364e-6	-100.2	9.7297e-6	-100.2	6.9821e-5	-83.12
T Loop #8	9.8553e-5	-80.13	9.3556e-5	-80.58	1.8654e-4	-74.58
Short T L #7	7.1695e-6	-102.9	7.1008e-6	-103	7.1759e-6	-102.9

By comparing the infinity-norm errors in Table 4-4, one can observe that the overall performance using the direct search method is better than the one obtained by using balanced realization method. The infinity-norm error on average is around -90dB in the former case while it is around -80dB in the latter case.

One can also find the reduced-order model by minimizing the 2-norm of the approximation error using the same direct search method. In this case, the least-squared error between the magnitude response of the original filter and that of the resultant

reduced-order model in minimized. The same experiment is performed by using Nelder-Mead simplex method in order to minimize the 2-norm of the approximation error. The results are shown in Table 4-5:

Table 4-5: Mean-squared error for all test loops using Nelder-Mead method

Test Loop	*Approximation Error*			
	Normal Search	dB	Weighted Search	dB
T Loop #7	1.2352e-7	-138.17	1.6848e-8	-155.47
T Loop #9	3.9622e-6	-108.04	3.9497e-8	-148.07
T Loop #13	2.9921e-6	-110.48	3.5739e-7	-128.94
C Loop #4	2.5877e-6	-111.74	2.2281e-7	-133.04
C Loop #6	3.1629e-6	-109.99	6.165e-10	-184.2
C Loop #7	4.0077e-6	-107.94	1.6244e-7	-135.79
C Loop #8	2.4758e-6	-112.13	1.6344e-7	-135.73
Mid-C Loop	2.6169e-6	-111.64	7.6489e-8	-142.33
C Loop #0	1.7523e-12	-235.13	5.4326e-13	-245.3
T Loop #1	1.86e-7	-134.61	8.7881e-10	-181.12
T Loop #2	6.1255e-7	-124.26	2.7977e-8	-151.06
T Loop #5	1.8498e-6	-114.66	5.0645e-8	-145.91
T Loop #8	6.7255e-8	-143.45	1.2597e-9	-177.99
Short T L #7	1.9226e-6	-114.32	4.1975e-9	-167.54

The 2-norm and infinity-norm error minimizations both lead to reduced order models with good accuracies. However, one should note that minimizing the 2-norm of error results in a model whose output deviation (with respect to the original system) has minimum power in the desired frequency range. Minimizing the infinity-norm, on the other hand, results in a model that maximum deviation of its output from the original system's output is minimized. The corresponding results can be more desirable when all frequency components of the output signal are to be reasonably close to those of the original output in the desired frequency range.

Chapter 5

5 Concluding Remarks

This chapter contains a summary of the work presented in the thesis. In addition some directions are proposed for future work.

5.1 Conclusions

With the vastly different possible DSL line configurations and undesirable effects of the bridge taps on the frequency response of the channel, it is important to have an estimation of the frequency characteristics of the distribution channel. Performance of the DSL service highly depends on the length and gauge of the segments of the main channel, the length and gauge of the bridge taps and their location, which all affect the frequency response of the channel. This is particularly important because DSL technology uses variable bit-rate signal processing technique over different frequency intervals.

It is hard to apply the necessary changes to the existing network infrastructure because the wired communication network is mainly an underground network. A reasonably precise model as a finite-dimensional LTI digital filter is useful in simulating

the entire network in a laboratory environment without disturbing the real customers by running experiments on the real network (which is sometimes done for trouble-shooting purposes). It also helps the DSL providers to verify the performance of the service before assigning it to the customer.

In this thesis, the magnitude response of DSL transmission line was approximated using both FIR and IIR digital filters. The order of the filter for any desired accuracy depends on the configuration of the line, and in particular on the bridge taps. It also depends on the filter type, i.e. for a given degree of accuracy, the order of the resultant IIR filter is smaller than that of the FIR counterpart. Thus, there is a trade-off between the accuracy of approximation and simplicity of the filter structure (in terms of the filter type and filter order). A computationally efficient recursive algorithm is also proposed to approximate the frequency response of the line with an IIR digital filter by using intermediate FIR filters.

There are several methods available to approximate a system with a FIR or IIR filter. The main problem is that some of these filters have high orders which makes it practically difficult to implement them as laboratory models. In many cases, depending on the network configuration, simplified models can have an acceptable accuracy in simulating the real system while they have less complexity and can be implemented easily.

One of the most effective techniques for model-order reduction is balanced realization. The tests performed on standard DSL loops show that the performance of this technique is much better than other existing methods.

Some standard DSL test loops are introduced and different model-order reduction methods have been performed on each of them. The accuracy of the proposed algorithm and that of the existing methods are compared in terms of the infinity norm of the error between the exact frequency response and the reduced-order models. The results are summarized in a table which gives useful information above the required digital filter order for any desired accuracy based on the physical characteristics of each loop.

5.2 Suggested Future Work

For future work in this field, it is recommended that the modeling takes the phase of the frequency response into account too, as the modeling proposed in this thesis takes only the magnitude response into account. It is also of interest to find a simple way to evaluate the infinity norm of an IIR filter with repeated poles (or at least find a bound on the ∞-norm in terms of filter coefficients) since it will speed up the infinity-norm estimation of IIR-FIR-IIR approximation proposed in section 4.3.

The modeling proposed in this thesis takes only one DSL channel into account. However, in practice the distribution cables carry more than one single DSL line. Therefore, there will be crosstalk effect between different DSL channels as discussed in sections 1.1.2 and 2.3.4. Thus, it will be useful to extend this work to multiple DSL channels and also to consider Far-End Crosstalk (FEXT) and Near-End Crosstalk (NEXT) so that the resultant model covers the whole bundle of DSL channels instead of just one of them.

Design of a local DSL network structure based on the available constraints and the practical limitations is another interesting topic to work on. The constraints can be directly related to the physical configuration such as the length of the cables used in the design, the number and the approximate place of bridge taps. It can also be related to the performance of the network such as the frequency response at the end-user nodes, etc.

Reference:

[1] A. C. Antoulas, S. Gugercin, "*On The Assignment of Eigenvalues in LTI Systems*", Proceedings of the 38th IEEE Conference on Decision and Control, vol. 1, December 1999, p. 486.

[2] A. Betser, E. Zeheb, "*Reduced Order IIR Approximation to FIR Digital Filters*", IEEE Transactions on Signal Processing, vol. 39, November 1991, pp. 2540-2544.

[3] A. E. Bryson, Y. C. Ho, *Applied Optimal Control*, Hemisphere Publishing, 1975, pp. 328-338.

[4] B. Beliczynski, I. Kale, G. D. Cain, "*Approximation of FIR by IIR Digital Filter: An Algorithm Based on Balanced Model Reduction*", IEEE Transactions on Signal Processing, vol. 40, no. 3, March 1992, pp. 532-542.

[5] N. A. Bruinsma, M. Steinbuch, "*A Fast Algorithm to Compute The H_∞-norm of A Transfer Function Matrix*", Systems and Control Letters, vol. 14, 1990, pp. 287 – 293

[6] R. H. Bartels, G. W. Stewart, "*Solution of the Matrix Equation $AX+XB=C$*", Comm. Of the ACM, vol. 15, no. 9, 1972.

[7] D. K. Cheng, *Field and Wave Electromagnetics*, 2nd edition, Addison Wesley, Menlo Park, CA, 1992.

[8] E. J. Davison, "*A Method For Simplifying Linear Dynamic Systems*", IEEE Transactions on Automatic Control, vol. 11, no. 1, February 1966, pp. 93-101.

[9] J. C. Doyle, K. Glover, P. P. Khargonekar, B. A. Francis, "*State-space Solutions to Standard H_2 and H_∞ Control Problems*", IEEE Transactions on Automatic Control, vol. 34, no. 8, August 1989, pp. 831 – 847.

[10] D. Enns, "*Model Reduction With Balanced Realization: An Error Bound And Frequency Weighted Generalization*", Proceedings of the IEEE Conference on Decision and Control, 1984, pp. 127-132.

[11] B. A. Francis, "A Course in H_∞ Control Theory," (Lecture Notes in Control and Information Sciences, Vol. 88), New York, Springer-Verlag, 1987.

[12] B. A. Francis, J. C. Doyle, "*Linear Control Theory With An H_∞ Optimality Criterion*", SIAM Journal Contr. Opt., vol. 25, 1987, pp. 815-844.

[13] B. Friedlander, B. Porat, "*The Modified Yule-Walker Method of ARMA Spectral Estimation*", IEEE Transactions on Aerospace Electronic Systems, vol. 20, no. 2, March 1984, pp. 158-173.

[14] G. Gu, "*All Optimal Hankel-Norm Approximations And Their L_∞ Error Bounds in Discrete-Time*", Proceedings of the 41st IEEE Conference on Decision and Control, vol. 4, December 2002, pp. 3742-3747.

[15] K. Glover, "*All optimal Hankel-norm approximations of linear multivariable systems and their -error bounds*", International Journal of Control, vol. 39, 1984, pp. 1115-1193.

[16] S. Gugercin, A. C. Antoulas, "*A Comparative Study of 7 Algorithms For Model Reduction*", Proceedings of the 39th IEEE Conference on Decision and Control, vol. 3, December 2000, pp. 2367 – 2372.

[17] F. J. Harris, "*On the Use of Windows for Harmonic Analysis with the Discrete Fourier Transform*" IEEE Proceedings, vol. 66, no. 1, January 1978, pp. 51-83.

[18] N. L. Hettiarachchi, A. A. Sakla, "*Design of Digital FIR Filters Via Optimized Generalized Reimann Window Function*", Proceedings of the 37th Midwest Symposium on Circuits and Systems, vol. 2, August 1994, pp. 1061 – 1064.

[19] ITU-T Recommendation G.992.1, Asymmetric Digital Subscriber Line (ADSL) Transceivers, 1999.

[20] ITU-T Recommendation G.992.2, Splitterless Asymmetric Digital Subscriber Line (ADSL) Transceivers, 1999.

[21] ITU-T Recommendation G.996.1, Test Procedures for Digital Subscriber Line (DSL) Transceivers, 1999.

[22] T. Kailath, *Linear Systems*, Prentice-Hall, 1980.

[23] A. J. Laub, "*Computation of Balancing Transformations*", Proceedings of American Control Conference, San Francisco, vol. 1, FA8-E, 1980.

[24] A. J. Laub, M. T. Heath, C. C. Paige, R. C. Ward, "*Computation of System Balancing Transformations and Other Applications of Simultaneous Diagonalization Algorithms*", IEEE Transactions on Automatic Control, vol. 32, no. 2, February 1987, pp. 115 – 122.

[25] J. C. Lagarias, J. A. Reeds, M. H. Wright, P. E. Wright, "*Convergence Properties of The Nelder-Mead Simplex Method in Low Dimensions*", SIAM Journal of Optimization, vol. 9, no. 1, 1998, pp. 112-147.

[26] B. Moore, "*Principal Component Analysis in Linear Systems: Controllability, Observability And Model Reduction*", IEEE Transactions on Automatic Control, vol. 26, no. 1, February 1981, pp. 17-31.

[27] A. V. Oppenheim, R. W. Schafer, J. R. Buck, *Digital Signal Processing*, Englewood Cliffs, NJ: Prentice-Hall, 2nd edition, 1999.

[28] A. V. Oppenheim, A. S. Willsky, S. H. Nawab, *Signals And Systems*, Upper Saddle River, NJ: Prentice-Hall, 2nd edition, 1996.

[29] K. Ogata, *Modern Control Engineering*, Englewood Cliffs, NJ: Prentice-Hall, 1990.

[30] L. Pasquato, I. Kale, "*Adaptive IIR Filter Initialization via Hybrid FIR/IIR Adaptive Filter Combination*", IEEE Transactions on Instrumentation And Measurement, vol. 50, no. 6, December 2001, pp. 1830-1835.

[31] L. Pasquato, I. Kale, "*Improved Convergence in the Sequential Regression Algorithm for the Adaptive Identification of IIR Systems*", Adaptive Systems for Signal Processing, Communications, and Control Symposium, October 2000, pp. 193-196.

[32] L. Pasquato, I. Kale, "*System Identification via Hybrid FIR-IIR Adaptive Filtering*", Instrumentation and Measurement Technology Conference, vol. 2, May 1999, pp. 1064-1069.

[33] L. Pernebo, L. M. Silverman, "*Model Reduction via Balanced State Space Representations*", IEEE Transactions on Automatic Control, vol. 27, no. 2, April 1982, pp. 382-387.

[34] T. Penzl, "*Eigenvalue Decay Bounds For Solutions of Lyapunov Equations: The Symmetric Case*", Systems and Control Letters, vol. 40, 2000, pp. 139 – 144.

[35] T. W. Parks, J. H. McClellan, "*Chebyshev Approximation for Nonrecursive Digital Filters with Linear Phase*", IEEE Transactions on Circuit Theory, vol. 19, no. 2, March 1972, pp. 189-194.

[36] W. D. Reeve, *Subscriber Loop Signaling and Transmission Handbook – Analog*, IEEE Press, New York, 1992.

[37] W. D. Reeve, *Subscriber Loop Signaling and Transmission Handbook – Digital*, IEEE Press, New York, 1995.

[38] T. Starr, J. M. Cioffi, *Understanding Digital Subscriber Line Technology*, Prentice Hall, Upper Saddle River, NJ, 1998.

[39] C. Valenti, "*Cable Crosstalk Parameters and Models*", ANSI Contribution T1E1.4/97-302, Bellcore, Minneapolis, MN, September 1997.

[40] J. J. Warner, "*The HDSL Environment*", IEEE Journal on Selected Areas in Communications, vol. 9, no. 6, August 1991, pp. 785-800.